12-2014

Characterization of GaN thin films grown by RF Magnetron Sputtering for fabrication of an AlGaN/GaN HEMT biosensor

Rocio Yolanda Garza
University of Texas-Pan American

Recommended Citation

CHARACTERIZATION OF GAN THIN FILMS GROWN BY RF

MAGNETRON SPUTTERING FOR FABRICATION OF AN

ALGAN/GAN HEMT BIOSENSOR

A Thesis

by

ROCIO YOLANDA GARZA

Submitted to the Graduate School of
The University of Texas-Pan American
In partial fulfillment of the requirements for the degree of

MASTER OF SCIENCE

December 2014

Major Subject: Electrical Engineering

CHARACTERIZATION OF GAN THIN FILMS GROWN BY RF

MAGNETRON SPUTTERING FOR FABRICATION OF AN

ALGAN/GAN HEMT BIOSENSOR

A Thesis
by
Rocio Yolanda Garza

COMMITTEE MEMBERS

Dr. Hasina Huq
Chair of Committee

Dr. Heinrich Foltz
Committee Member

Dr. Karen Lozano
Committee Member

December 2014

ABSTRACT

Garza, Rocio Y., <u>Characterization of GaN Thin Films Grown by RF Magnetron Sputtering for Fabrication of an AlGaN/GaN HEMT Biosensor</u>. Master of Science (MS), December, 2014, 87 pp., 17 tables, 59 figures, 54 references, 56 titles.

Radio-Frequency (RF) Magnetron Sputtering has been used to grow GaN thin films for future fabrication of an AlGaN/GaN HEMT biosensor. A GaN target was sputtered at various parameters on silicon and sapphire substrates, at room temperature and at elevated temperature using substrate heating and post deposition annealing treatment. The research conducted investigates the effects of sputtering gas (Argon or Nitrogen gas), RF power (40W or 50W), and pressure (4mT − 30mT) on the structural properties of the thin films. Imaging tools such as the Atomic Force Microscopy (AFM), Scanning Electron Microscopy (SEM), Energy-dispersive X-ray spectroscopy (EDS), X-ray Diffractometer (XRD), and X-ray photoelectron spectroscopy (XPS) are used for characterization of each thin film. Results revealed that polycrystalline GaN thin film with a hexagonal GaN wurtzite structure can be grown on silicon and sapphire wafers. In addition, oxygen impurities incorporated during the deposition are shown to be reduced by using temperature depositions.

DEDICATION

This Thesis studies would not have been possible without the love and support of my family, my mother, Lourdes Mantecon-Garza, my father, Jesus Miguel Garza, my sisters, Maria Laura, Alejandra, Maria de Lourdes, and Sofia del Roble. These individuals helped me in the completion of this project and encouraged me to accomplish this degree. Thank you for your love, patience and pushing me to achieve my goals.

ACKNOWLEDGMENTS

TABLE OF CONTENTS

<div align="right">Page</div>

LIST OF TABLES

LIST OF FIGURES

CHAPTER I

INTRODUCTION

In the last 50 years, technology has advanced at a rapid pace improving society through medical breakthroughs, rapid communications, and faster, more efficient methods of doing things. Since the development of the transistor in 1947, a reduction in size and increase in capabilities of electronic components has been achieved [1]. This lead the transistor to become the building block of modern electronic hardware. Transistors are essential to create integrated circuits that are found in various household appliances such as cell phones, computers, TVs and other electronic devices used every day. Without transistors, these devices would be slow and bulky and/or possibly nonexistent. Today, a single computer chip can contain billions of transistors and Moore's law (the prediction that the number of transistors placed on a single chip would double every 1.5 to 2 years), still holds true [2]. A variety of commonly used transistors exist such as, bipolar-junction transistors (BJTs), metal–oxide–semiconductor field-effect transistor (MOSFET) and metal–semiconductor field effect transistor (MESFET), with each one consisting of different structures and material components that are best suited for their applications.

Recently, much attention has been given to the use of transistor devices for sensing applications in the fields of biology, chemistry and medicine for homeland security, medical and environmental monitoring [3]. Biosensors are used as analytical instruments for the detection of biological and chemical analytes. These biosensors are capable of detecting/recognizing

1

biological responses that are amplified and converted to a measurable electrical signal [3]. As reported by (Kang et al., 2008), the global sensor market has increased significantly in the previous decade, with an expected $61.4 billion value by 2010. The types of materials for sensor applications are termed "smart materials" in that they are sensitive to changes in the environment such a as temperatures, electric fields and gasses and can instantly respond to these changes in predetermined manner. Advances in transistor technology and newer fabrication methods create the possibility of micro sized bio sensors with advantages including: small size and weight, faster response time, and better reliability. Additionally, low cost mass production, and integration into wireless sensor networks for remote monitoring which in some instances can be used in in-vivo operation for real time feedback [4] can be possible.

The Aluminum Gallium Nitride/ Gallium Nitride High Electron Mobility Transistor (AlGaN/GaN HEMT) was selected for this research work because it is a type of transistor that has the capabilities to be a highly suitable bio sensor. AlGaN/GaN HEMTs have high resistance to corrosion by acids, non-toxicity to living cells, extreme sensitive detection, ability to work in harsh environments and are chemically inert. Their unique characteristics have already shown great potential as a future analytical instrument, where silicon based field effect transistors (FETs) biosensors have been ineffective [3].

1.1 Semiconductor Materials and Devices

Transistor devices would not be possible without semiconductor materials. Semiconductors are unique materials that have the electrical conductivity between that of a metal and insulator, and most importantly they have the capacity to be altered to be more conductive or insulating. However, limitations exist on how much semiconductors can be altered by the intrinsic properties of the material [5]. Thus, a transistor's performance can be restricted or

advanced by the semiconductor material(s) it is made of. Traditionally, the primary material for transistors has been dominated by the semiconductor material silicon (Si), due to its low cost, reproducibility, and abundance [6]. As new applications emerge, limitations such as speed and poor thermal capacity are being reached where current Si technology cannot keep up with emerging market demands [7]. A material's electrical conductivity is dependent on the atomic arraignment of its atoms, and Si based devices are already being pushed to the capacities exhibited by their material properties. To overcome current Si limitations, new state of the art materials are being researched.

Group III-V semiconductor compounds have material properties that allow the potential for higher speed operation than silicon-based devices. By utilizing group III-V semiconductor compounds, devices can be smaller, more efficient and work in harsher environments [8]. Despite the benefits, these semiconductors commercial sale is limited, as the cost is 3 to 5 times higher than silicon [9]. Gallium Arsenide (GaAs) was one of the first group III-V semiconductor materials to be commercially used exhibiting great advantages over Si. However, the group III-V semiconductor compound Gallium nitride (GaN) has material properties superior to both Si and GaAs. GaN's high carrier mobility and its ability to operate at much higher temperatures and voltages, has made it a main topic of research for next generation technologies [7] [10] [11]. Advantages of GaN material properties over other semiconductor materials can be seen on Table 1.1.

Table 1.1 - Properties of (300K) select semiconductors vs GaN [12]

Attribute	Si	GaAs	4H-SiC	GaN
Energy Gap (eV)	1.12	1.42	3.25	3.25
Breakdown E-Field (V/cm)	0.25	0.4	3.0	3.0
Electron Mobility $\mu(cm^2/V*s)$	1350	6000	800	800
Thermal Conductivity (W/cm*K)	1.5	0.5	4.9	4.9
Dielectric constant ε	11.8	12.8	9.7	9.7

1.1.1   Applications of GaN Devices

GaN devices were first utilized in bright Light Emitting Diodes (LEDs), optoelectronics, high power and high frequency devices in the fields of microwave and power electronics [7] [13]. Recently, the 2014 Nobel Prize was awarded for the invention of efficient bright blue LEDs which are white light sources that will reduce energy fabricated using GaN [14]. The competitive advantages and outperformance of conventional transistors of GaN has increased interest in commercial and military applications. Current market demands for GaN electronic devices is expected to increase by the end of this decade [13]. Furthermore, GaN chemical inertness and piezoelectric properties make it ideal for bio sensing applications. For these reasons, AlGaN/GaN HEMTs have emerged as powerful devices and gotten a lot of attention in bio-sensing applications.

HEMT technology come from the family of field effect transistor (FET) devices, which use the electric field to control the flow of current through the device [15]. It is advantageous since the free carrier concentration within the semiconductor layer can be increased significantly without introduction of dopant impurities [6]. The first HEMT device was an Aluminum Gallium Arsenide/ Gallium Arsenide (AlGaAs/GaAs) HEMT. GaAs costs less and is much easier to fabricate. However, GaN HEMTs have undeniable advantages for high power and high frequency applications than GaAs HEMTs. The high heat capacity allows operation of higher voltages without the need for an external cooling device. Furthermore, GaN HEMTs have high thermal conductivity, high breakdown voltage, and resistance to chemically hostile environments [16].

The advantages of HEMT technology to achieve high direct current (DC) and high radio frequency (RF) currents comes from the creation of a two-dimensional electron gas (2DEG). The

2DEG is created when two distinct semiconductors with different band gaps are grown on top of one another, creating a heterojunction. The heterojunction created from AlGaN/GaN generates a current flow with very high mobility (~1200 – 1500 cm^2/ (Vs)), and allows for modulation doping, the addition of impurity atoms to control the behavior of the HEMT [6]. However, this is not always necessary as the heterojunction's electron mobility is already efficient. Furthermore, the close proximity of the heterojunction to the surface (<35nm) makes the device extremely sensitive to the ambient changes due to the surface charges and results in greater sensitivity detection [17].

AlGaN/GaN HEMT high sensitivity can be used to achieve simultaneous detection of a variety of environmental and biological gasses and liquids [18]. Its high-sensitivity, label-free and real time detection can also be utilized in DNA sequencing and targeted biological markers. It can be an important aspect in medicine due to its ability to detect abnormalities in the body sooner and in a less invasive way [3] [17]). Detection of targeted markers is possible by adding a liquid sample on the gate of an AlGaN/GaN HEMT. A large change in the source-drain current can then be observed, which can be interpreted as an electrical signal representation of the biological solution [17].

1.1.2 Structure of AlGaN/GaN HEMTs

The typical structure of the device includes three external electrodes: source, drain and gate, AlGaN barrier, 2DEG channel layer, and GaN layer (Figure 1). GaN HEMTs have been grown using the substrate materials Si, sapphire and Silicon Carbide (SiC). Choosing the right substrate is essential as the characteristics and capabilities of the substrate material can affect its performance. Growing two different materials on top of each other requires a certain compatibility of the property of the two materials, and it is needed in order to grow high quality

layers. The thermal conductivity and the lattice match are critical to reduce stress and to achieve high quality crystals. For this reason, a nucleation layer is sometimes used between GaN and the substrate material to compensate mismatch [13]. More information on the substrates used will be given in Chapter 2.
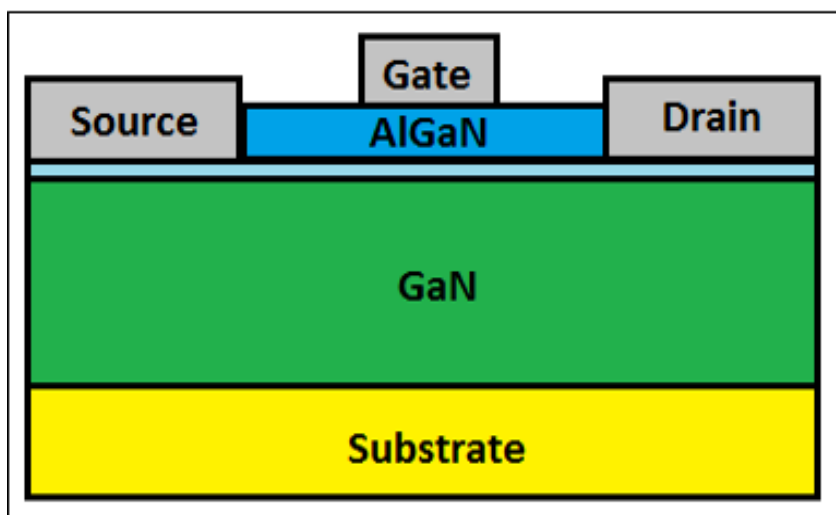
Figure 1.1 - Basic AlGaN/GaN schematic

1.1.3 Challenges Limiting Commercialization of GaN Devices

Compound semiconductors have not been as widely used for commercial applications as Si, as they tend to be more fragile and are more difficult to grow [10]. Fabrication cost and the number of defects in the crystal are higher. The growth of compound semiconductors possess challenges not found in elemental compounds due to the atomic positioning of the molecules called a "crystal structure" [8]. The crystal structure is an arrangement in space of atoms, ions, and molecules found in solids. An elemental semiconductor's atomic arrangement will consist of only one kind of atom in its crystal structure. Compound semiconductors are comprised of several elements [5]. These crystal structures are formed due to the arrangement of atoms of different groups. The term "crystal lattice" is given to a 3-dimentional array of points in space pertaining to the position of where the atom lies within the crystal structure [10]. When growing

6

compound semiconductors, control of the ratio of the two elements (stoichiometry) is essential. For instance, a gallium (Ga) atom must reside on a Ga site and not on a nitrogen (N) site, and vice versa. This is in contrast to growing single element elemental semiconductors, because the position of the site is not relevant, making them easier to grow [8]. All of these factors have limited the commercial use and sale of compound semiconductors. However, because of the superior fundamental material properties of compound semiconductors over Si, research has pushed for a low cost and more feasible manufacturing techniques.

Although GaN devices have unquestionable advantages, they are compound semiconductors and, as such, they have not been popularized due to fabrication issues. GaN material does not exist purely in nature and device performance is limited by difficulties in growing high quality GaN. Until the 1990s, the absence of reliable processing procedures, compatible substrates, and lack of high quality GaN resulted in this semiconductor being ignored, falling behind to other semiconductors such as silicon which is cheap and reliable [12].

1.2 Fabrication of an AlGaN/GaN HEMT

A transistor is made of various types of conductor, semiconductor and insulator thin film layers on a wafer, also called a substrate. Deposition, Pattering, and Etching of the multiple layers of transistors are basic requirements for fabrication (Figure 1.2). Each processing step is complex and requires careful study. This thesis involves only the thin film deposition of GaN, which is one of the basic materials of the desired HEMT biosensor. Thin film is a term used on layer thicknesses in the nanometer scales, typically less than 0.5microns [19]. Deposition techniques of thin film involve the growth of nano scale layers of a material onto a substrate. In this process, thin film layers are created by the addition of each individual atom, until a desired thickness is achieved.
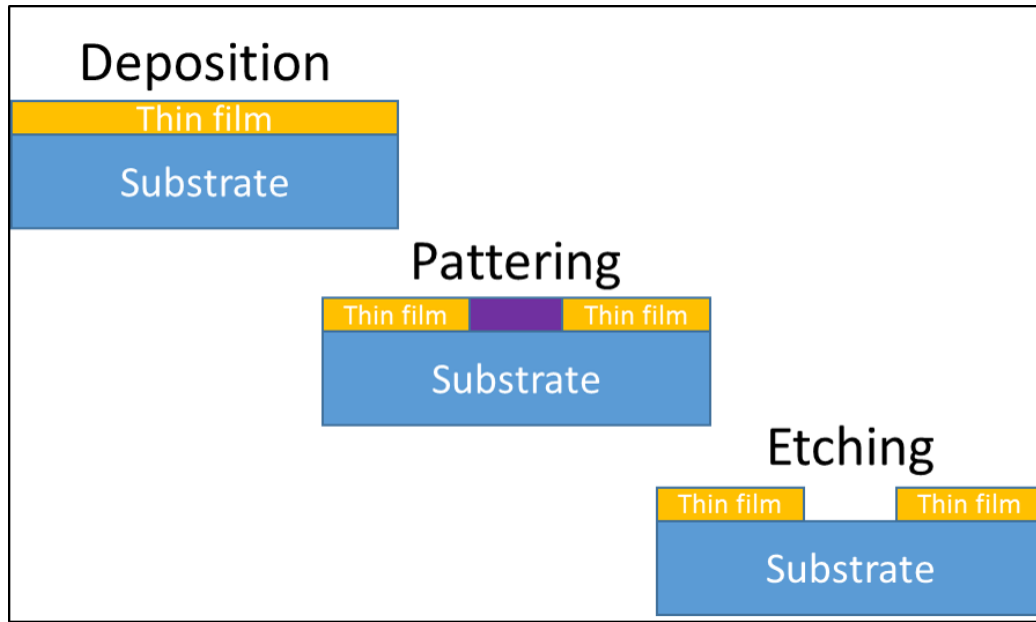
Figure 1.2 - Fabrication process

1.3 Thin Film Deposition

Thin film deposition methods can be categorized as either chemical vapor deposition (CVD) or physical vapor deposition (PVD) (Figure 1.3). As can be understood by its name, CVD uses chemical reactions to decompose the target material and deposit thin film. In this process, the gas phase reactants are introduced in the main chamber at room temperature. When it comes in contact with a heated substrate, the reactants will react and the desired solid material is formed. The important parameter is the substrate temperature, as it will influence the reactions taking place. As opposed to CVD, PVDs use no chemical reaction but purely physical processes. In PVD, the solid material transitions to a gas phase and the atoms are evaporated on to the substrate. The type of deposition used generally depends on the application [20] [21] [22].

<div align="center">(a)   (b)</div>
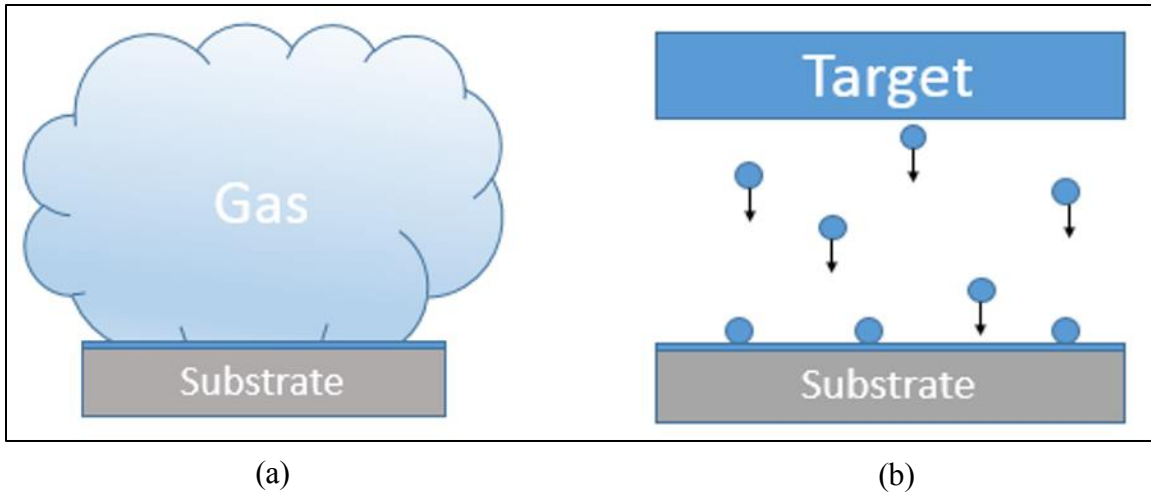
Figure 1.3 - (a) Chemical vapor deposition and (b) physical vapor deposition

Metal Organic Chemical Vapor Deposition and Plasma-Enhanced Chemical Vapor Deposition as well as molecular beam epitaxy and sputter deposition (both PVD) have proven to be successful for achieving single crystal GaN thin film [22]. Despite these demonstrations, these processes still face issues and/or limitations related to cost, complexity, involve corrosive elements, and require high temperature depositions. Furthermore, these methods leave defects due to the impurities of the GaN material [12]. However, the sputtering method is a PVD that is increasing in popularity due to its ease of operation of deposition systems, thickness control, and ability to deposit at lower temperatures [23]. Advances in sputtering systems have helped overcome previous fabrication defects. In this thesis, the research of GaN thin film deposition is extended by experimenting with sputtering of GaN, an emerging, inexpensive, physical vapor deposition technique that is already showing promising results.

1.4 Sputtering Deposition

The sputter deposition method is the erosion of a target solid onto a substrate. As shown in Figure 1.4, the process involves: 1) the bombardment of ionized gas molecules against a target

material, causing the atoms of the target to dislodge and move freely 2) the sputtered atoms then moves freely until collision with another object, typically a substrate or a wafer, and settling at the surface creating thin film [24].
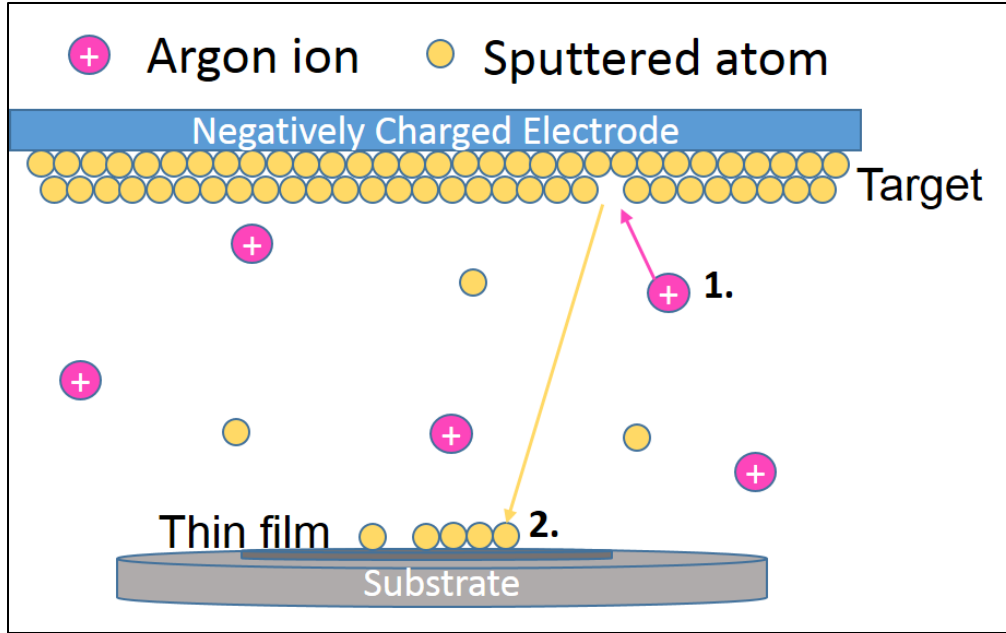
Figure 1.4 - Sputtering Process

Advantages of the sputtering method include: ease of operation, thickness control, low temperature deposition, and less toxicity [25]. There are several methods to grow GaN thin film, and the sputtering deposition is one of them. In the case of GaN thin film fabrication, both chemical (CVD) and physical (PVD) processes have been subjects of research.

1.5 Research and Outline

The purpose of this thesis is to extend the research for fabrication of AlGaN/GaN HEMT biosensors utilizing the sputtering method. Optimized sputtering conditions of GaN thin films are investigated experimentally for the preparation of an AlGaN/GaN heterostructure by RF magnetron sputter technique. The effects of sputtering power, temperature, gasses and pressure

are varied to study the effects on the structural properties of the thin films. Furthermore, semiconductor materials such as silicon, and sapphire are used as substrate materials to investigate the effects of substrate materials. This will then lead to the fabrication of an AlGaN/GaN HEMT biosensor (Figure 1.5).
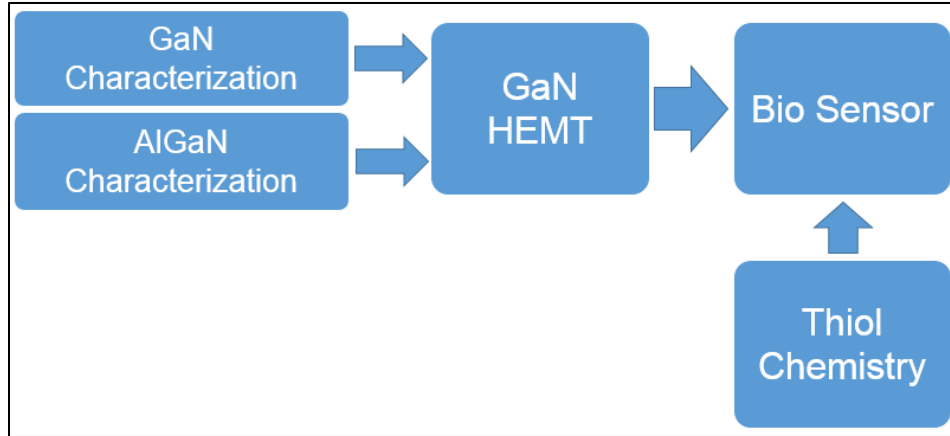
Figure 1.5 – Overall research outline

Chapter 1: Introduction to GaN material and devices. This will also describe the importance of AlGaN/GaN HEMT biosensors and introduce techniques for preparing thin films. It will focus on describing the sputtering method to familiarize the readers with the method. Finally, an outline of the overall research is presented.

Chapter 2: Semiconductor fundaments, crystallography and material properties will be described. The GaN material properties will be given as well as a brief reference to the AlGaN material for preparation of the AlGaN/GaN heterostructure. The substrate materials of Si, and Sapphire will also be described. Growth methods for GaN thin films are discussed as well as the importance of the chosen sputtering parameters.

Chapter 3: Methodology, the experimental procedures are described in chapter 3. Target and substrate preparation techniques as well as the characterization techniques are described. The experiment parameters are listed in the tables.

Chapter 4: Experimental Results for the preliminary depositions are described. This chapter focuses on preliminary results found using the sputtering machine, the experience gained and the verification of the functionality of the system.

Chapter 5: Experimental Results for the GaN depositions are given in the chapter. The results are explained through the different parameters used in sputtering from 0% nitrogen gas (using only argon gas) to using a mixed argon/nitrogen gas with increasing concentrations of nitrogen and finally using pure nitrogen depositions.

Chapter 6: Conclusion and Future Works, this chapter gives a brief summary of the findings of this thesis. Challenges are also discussed. Finally, recommendations are given for continuation of the research objective.

CHAPTER II

SEMICONDUCTOR PROPERTIES AND GROWTH TECHNIQUES

In this chapter fundamental properties of semiconductors is given for the understanding of the material properties that make semiconductors highly suitable for electronic applications. The structure and the material properties of GaN, AlGaN and substrates used as well as the epitaxial growth methods commonly used to grow epitaxial GaN are discussed.

2.1 Semiconductor Fundamentals

Semiconductor materials have revolutionized electronic circuits because they have unique material properties that make them ideal for electronics. The behavior of the atoms in semiconductor solids allow them to have the electrical properties between that of a metal and an insulator. Two important characteristics semiconductors possess are: 1) the electrical behavior is extremely sensitive to even the smallest concentration of impurity atoms, allowing the conductivity to be modulated through a controlled process called "doping" and 2) the electrical conductivity increases with increasing temperatures [8].

Semiconductor materials can be found in group III-V elements of the periodic table. Most can be characterized as elemental semiconductor materials, pertaining to group IV of the periodic table, and compound semiconductor materials, which are mostly combinations of group III and group V elements (called III-V semiconductors) [26]. To understand the material properties in semiconductors and how they relate to electrical conductivity, one must study the geometrical
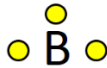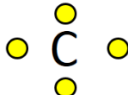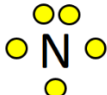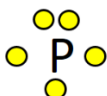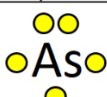
atomic arrangements and the interactions between atoms and molecules bonded together to make a solid. The Bohr model can be used to for the interpretation of an atom. An atom consists of a nucleus surrounded by an equal amount of electrons and protons (Figure 2.1). The electrons are negative carriers and the protons are positive carries (holes). Each group number on the period table pertains to the number of electrons orbiting in the outmost shell called the valence shell around the nucleus. Those of group II have two electrons, group III have three electrons etc. Good conductors have "free electrons" in their valance shell that permit atoms to easily move, allowing the flow of electricity. Insulators have all the electrons in their valence shell in covalent bonds (two atoms sharing one electron), and the electrons are restricted to this region and are not free to move. In the case of semiconductors, a poor conducting semiconductor like silicon can be altered to behave like a conductor through doping. Other factors such as the type of material or mixtures (compound semiconductors) can also affect how much electricity it can conduct [5] [10] [26].
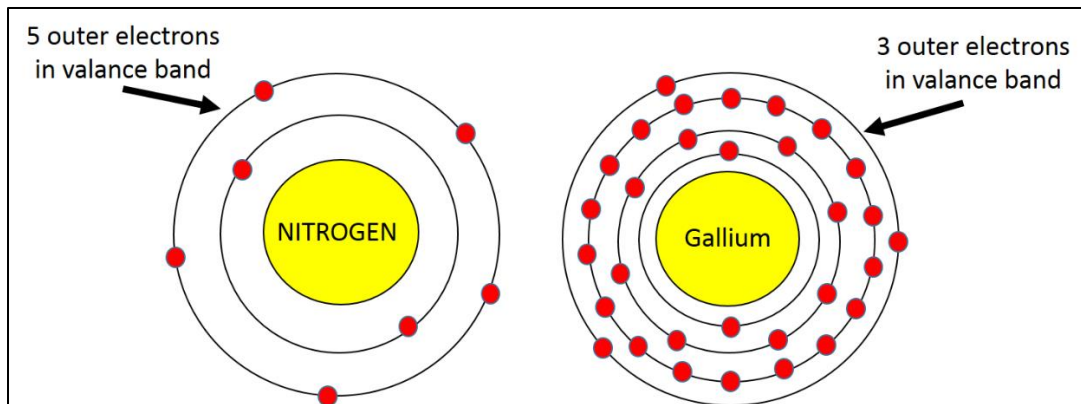
Figure 2.1 - Bohr models of nitrogen and gallium

The number of electrons in the valence shell is an important characteristic as it determines how the atom behaves in chemical reactions. Atoms bond due to the tendency to fill up their outermost electron shell and become more stable [10]. In group III-V compounds, the

14

lower level group III become acceptors and upper level group V elements become donors, as the low level element will accept a donor electron from the higher level group element. A section of the periodic table with commonly used elements and their outer electrons is shown in Figure 2.2. There can also be a ternary (3) or quaternary (4) compounds. Figure 2.3 shows common elemental and compound semiconductors. Properties of semiconductors vary because semiconductor materials come from different groups in the periodic table. As these compounds exhibit superior material properties than elemental group IV semiconductors [5]. The semiconductor materials discussed in this thesis pertain to group III-V compound materials, gallium nitride (GaN) and aluminum gallium nitride (AlGaN).

Figure 2.2 - Select elements from the periodic table
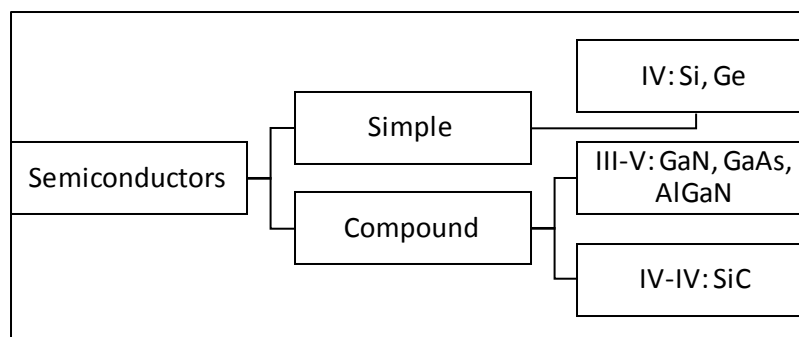
Figure 2.3 - Semiconductors by group

2.2 Semiconductor Crystal Structures

Semiconductor materials can be classified by the crystallography, the study of the arrangement of atoms within a solid. There are three types of solid crystal structures: amorphous, polycrystalline or crystalline. Each category is determined by the size of the ordered region where atoms or molecules have a periodic pattern arrangement. If the atoms are randomly placed and have no repeating patterns, they are non-crystalline or amorphous. If there are regions with a high degree of order (single crystal) varying in size and orientation, they are polycrystalline. The ordered regions are called grains and grain boundaries are made where the various sized single-crystal regions meet. If there is one highly ordered repeating pattern, then it is single crystal or crystalline, Figure 2.4. The atoms of single crystal materials have a group of atoms repeating periodically, this periodic arrangement in the crystal is called the lattice or crystal structure. Generally, single crystal materials have superior electrical conductivity than the others, due to the tendency of the grain boundaries to degrade the electrical characteristics. In a wafer, the orientation and the atomic arrangement depends on the manufacturing process [5] [10].

(a)   (b)   (c)
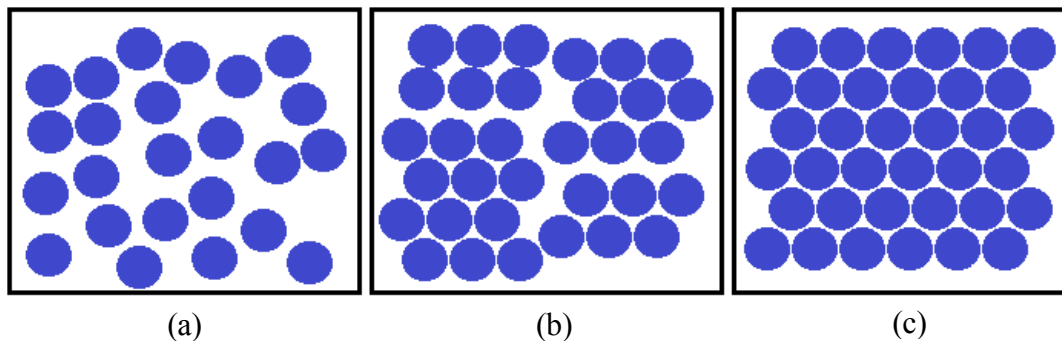
Figure 2.4 – (a) amorphous, (b) polycrystalline, and (c) crystalline atom arrangement

2.3 Properties of Semiconductors: Band gap

The band gap can provide an explanation for the useful properties of semiconductors that insulators and conductors do not have. The band gap is the energy difference between the top of the valance band and the bottom of the conduction band. Free electrons reside in the conduction band and the valance band consists of the electrons in the outermost orbit of atoms. The band gap is based on the fact that an electron can jump from the valance band (low energy state) to the conduction band (high energy state) and vice versa. An electron will always be at either of the two distinct energy states, with the minimum energy required to be at the high energy state and "break free" to become a charge carrier is called the "band gap". The band gap in good conductors like copper does not exist and the energy bands overlap. Insulators have a wide band gap so wide, that the electrons do not have enough energy to move from the valance band to the conduction band. Semiconductors have a band gap between that of a metal and an insulator and electrons can gain enough energy to jump (Figure 2.5). Furthermore, temperature has an effect on the energy, and can turn a semiconductor device ON. At low temperatures, covalence bonds stay in place, and semiconductors act like insulators. At high temperatures, the electrons gain enough energy to break away from their covalent bond and are able to move freely and conduct. Thus, the band gap gives measure to the electrical conductivity of the material. The number of the free electrons in the conduction band "free carrier concentration" and energy is the basic operation of electronic devices [5] [27].
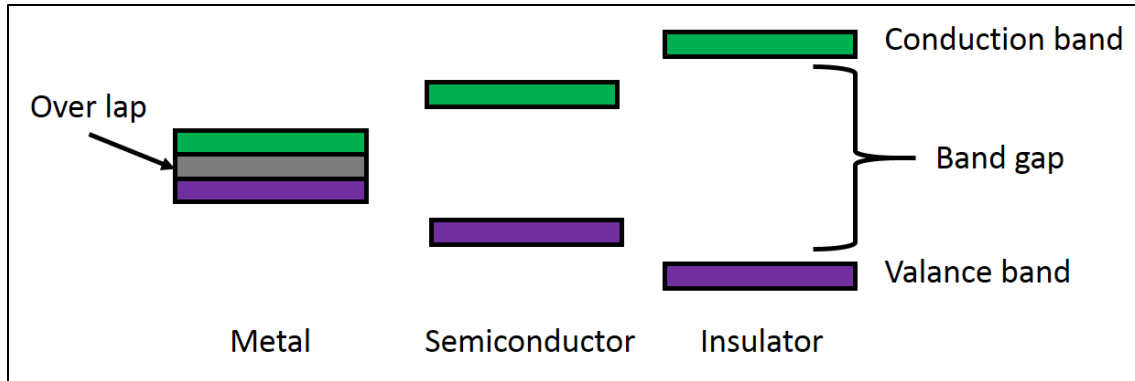
Figure 2.5 - Difference in band gap energies of metal, semiconductors and insulators

Wide band gap (WBG) semiconductors can be categorized as having much wider band gaps than Si (1.1eV). Silicon carbide (SiC), GaN and diamond are the top three materials with the highest band gaps of all semiconductors, with 3.26eV, 3.4eV, and 3.6eV, respectively [16]. A comparison of commonly used semiconductors band gaps are shown on Table 2.1. The material properties of WBG semiconductors enable smaller and faster devices, while operating at higher frequencies, voltages and temperatures and reduced power consumption than Si devices [7]. The semiconductors and band gaps of select semiconductors are shown in Table 2.1.

Table 2.1 - Elemental and Compound semiconductors

Elemental semiconductor	Symbol	Group	Band Gap (eV)
Silicon	Si	Group IV Elemental	1.1
Gallium arsenide	GaAs	Group III-V Compound	1.4
Silicon carbide	6H-SiC	Group III-V Compound	3
Gallium nitride	GaN	Group III-V Compound	3.4
Aluminum gallium nitride	AlGaN	Group III-V Compound	3.4
Diamond	C	Group IV Elemental	5.5

2.4 Structural and Material Properties of Gallium Nitride

As introduced in Chapter 1, GaN is a part of the group III nitrides such as AIN and InN, which have superior material properties like wide band gap and chemical inertness, than conventional semiconductors. Growth of high quality single crystals is difficult for any of the group III nitrides, but research procedures for growing bulk single crystals and thin film of GaN dates back to 60s [28] [12]. GaN crystalizes in three structures, zinc-blend, wurtzite and rock-salt [21]. The focus of this thesis will be only on the blende (cubic structure β phase) and wurtzite (hexagonal structure α phase) as they exhibit the electrical properties necessary for this thesis (Figure 2.5). The type of crystal grown is greatly affected by the growth procedures, parameters and conditions. Generally, wurtzite GaN is the preferred structure, as it has a wider band gap (3.5eV) than zincblende (3.3eV) [10] [16] [29] [30].
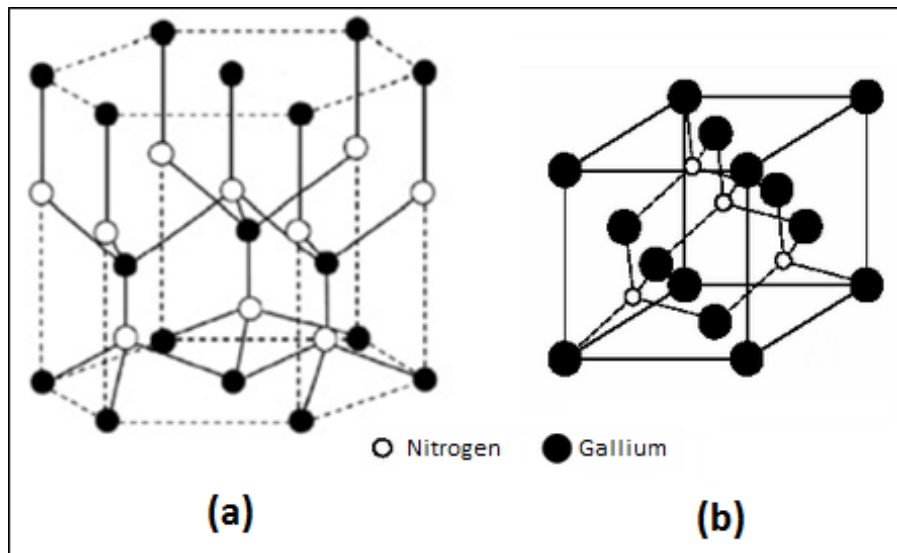
Figure 2.6 - (a) Hexagonal wurtzite *[16]* and (b) zincblende GaN *[30]*

The band structure of wurtzite and zincblende GaN have direct energy band gaps. At room temperature GaN has a wide band gap of 3.44eV [21]. Its large energy gap can support a high internal electric field (Ec) and a low dielectric constant. Its high carrier mobility is able to achieve higher currents than SiC and GaAs, which have a lower mobility. In addition, a high power density of 10-12W/mm of gate periphery can be achieved. GaN's thermal conductivity is 1.2W/cm, however different substrate materials can increase the thermal conductivity such as SiC and sapphire. Table 2.2 summarizes the material properties of GaN [12] [11].

Table 2.2 - Properties of GaN

Properties	
Molecular Formula	GaN
Melting point	>2500°C
Band gap	3.44eV
Electron mobility	440 cm²/(V·s) (300 K)
Thermal Conductivity	2.3 W/(cm·K) (300 K)
Breakdown field	~5x10⁶ (Vcm⁻¹)

2.4.1 AlGaN/GaN Heterostructure

Preparation of an AlGaN/GaN heterostructure is the second goal in the overall research. The heterostructure is the foundation of building the HEMT. Heterostructures allow a much higher increase in carrier mobility, due to the formation of the 2 dimensional electron gas (2DEG) at the heterostructure junction. First reports of the (2DEG) created by the heterojunction date back to 1991 [11]. The 2DEG allows for modulation doping, high saturation velocity, high carrier mobility and a reduction in ionized impurity scattering. Since then, many reports have proven its high power operation, high temperature and sensing applications [6] [7] [16]. In GaN-based heterostructures, a high electron concentration of ns 10^{13} cm^{-2} is achieved without the need for dopant impurities (modulation doping), induced by the spontaneous and piezoelectric

polarization. A conducting channel is formed, called 2DEG, and tightly confines electrons in a triangular quantum well, generating the high mobility. Additionally, the close proximity of the layer to the surface, results in very sensitive sensors for detection of gases, chemicals, pressure changes and biological species [12] [31].

Modulation doping is possible by the difference in band gaps of the two materials. When a semiconductor with a wider band gap (higher energy state) is grown on top of one with a narrow (lower energy state) band gap, the electrons will occupy the lowest energy state (Figure 2.6). In the AlGaN/GaN heterostructure, electrons will move from the AlGaN to GaN and an increase in carrier concentration of electrons on GaN is achieved without the need to introduce donor impurities. Positive donor charges left behind in Al, will balance out negative charge from the transfer, creating the higher electron mobility. As can be seen from figure 2.7, the band structure left is complex. The electron transfer results in the energy of electrons in the conduction band to bent in GaN. Electrons are confined in a triangular sub band potential well, generating the 2DEG [32].
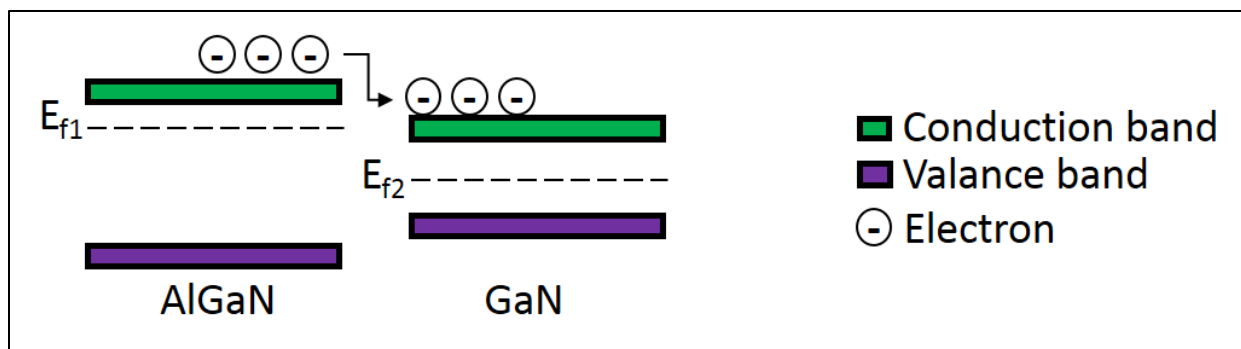
Figure 2.7 - Electron transfer between a wide band gap (AlGaN) grown on a narrow band gap (GaN) semiconductor creating modulation doping
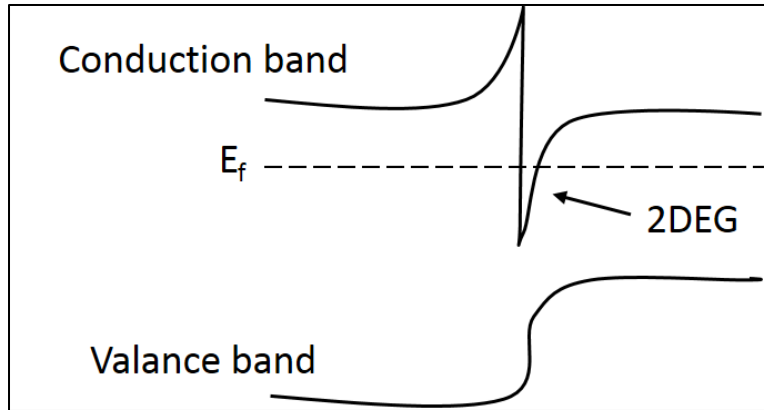
Figure 2.8 - Energy band diagram left after electron transfer

Polarization is beneficial in GaN HEMTs as it gives rise to 2DEG sheet concentrations larger than is possible with conventional III-V systems [29]. The two types of polarization effects are seen due to discontinuities in spontaneous polarization and piezoelectric polarization between the layers. The polarization discontinuity gives rise to a significant positive fixed charge Spontaneous Polarization (PSP), is the built in polarization field present in an unstrained crystal, which is exhibited by each individual AlGaN and GaN material. Piezoelectric Polarization (PPE) results from distortion of the crystal lattice when AlGaN and GaN are grown on top of each other, and PPE is exhibited on the AlGaN layer. The distortion of the crystal lattice comes from the two different crystal lattices of GaN and AlGaN. AlGaN's wider lattice has to accommodate to GaN's narrow lattice. The atoms are at different distances from each other and are being strained to accommodate the narrow layer. The offsets of the atoms generate an electric field [32].

2.4.2 Substrate Dependence on GaN Material Quality

As previously mentioned, choosing the right substrate greatly affects the efficiency of the HEMT device. Previous efforts for producing high quality GaN were not possible due to lack of suitable matching substrates. Although GaN substrates been recently become, they are expensive. Thus, a search for low-cost and suitable substrates for growing high quality GaN is underway. Material factors such as the cleanness of the substrate's surface, its quality and surface roughness can affect the surface roughness of the thin film, depleting its quality. Additionally, a higher output impedance, and good thermal properties are dependent on the physical properties of the substrate. The substrate can also impact crystallization of the thin film. Lattice mismatch between substrate and target have the greatest impact, and poor matching substrates can lead to strain or bad adhesion of sputtered atoms to the substrate from occurring [29]. GaN thin films grown on substrates with oriented plane of (0001) have been the choice for growing high quality GaN [29]. Diamond has the best thermal conductivity, creating GaN HEMTs with superior characteristics, but it comes at a high cost. Thus, (0001) oriented sapphire and SiC have been the substrates of choice for growing GaN. Sapphire is a lower cost substrate than SiC, however it has a high melting point and creates defects in the grown GaN layer. SiC has high thermal conductivity and can achieve greater high-power performance and thermal management, but it produces strain on the grown GaN crystal structure. Lately, Si has been of interest as a low cost substrate, but a nucleation layer was previously required due to lattice mismatch. Only recently has high quality GaN been grown on Si without the need for a nucleation layer or on different oriented substrates than (0001) due to advances in deposition techniques and nucleation schemes [12] [33].

Table 2.3 - Substrate lattice constant and coefficient of thermal expansion *[34]*

Substrate	GaN	Si <111>	Sapphire (Crystal of Al2O3)	SiC 6H
Lattice Constant (Å)	3.19	3.84	2.75	3.08
Coefficient of Thermal Expansion (CTE)	5.6	2.6	7.5	4.2

2.5 Growth Techniques

The structural properties of thin films are strongly dependent upon the deposition process and the growth parameters. Additionally, achieving good crystal structure reduces defects in material. Thus, fabrication of thin films has been extensively studied and a wide variety of growth techniques exist. Previously, growing high quality nitride based devices required expensive and complex processes such as Chemical Vapor Deposition (CVD), Metal-Organic Chemical Vapor Deposition (MOCVD) [35], and Molecular Beam Epitaxy (MBE) [33], as well as sputtering and evaporation [21] [12] [29]. Although epitaxial growth of GaN was achieved, material defects were still seen due to impurities of the GaN bulk material. Advances in state of the art systems such as sputtering, and availability of high purity GaN targets, has allowed more controlled, high quality films [12]. Recent reports (from 1999 and on) have shown R.F Sputtering of GaN has achieved polycrystalline and single crystal GaN by sputtering of a GaN target [36] [37] [38] [39] [40], a Ga target [41] [42] [43], and GaN powder target [44] [45] [46]. The resent reports of low substrate temperature procedures using RF magnetron sputtering has brought attention to sputtering. Use of this technique allows deposition on a variety of different substrate materials, large area depositions and low temperature growth. There is also the added ease of operation, thickness control, low cost, and less toxicity than previous popular methods [47].

2.5.1   Sputtering

The sputter method is a physical vapor deposition that can be traced back to the nineteenth century, but had not been widely used [8]. The sputter deposition method is a physical vapor deposition, under ultra-high vacuum pressure that is less than 10^{-9} mbar. This method for deposition is advantageous for its low cost, ease of deposition and sequential deposition, ability to control thickness, low temperature rating, and ability to grow thin films with the elimination of toxic gases. In this process, an inert gas like that of Argon or nitrogen, is introduced into a vacuum chamber. When a chamber pressure of $\sim 10^{-7}$ Torr is reached, the gas molecules transition into a state of plasma. Under plasma, the gas molecules are ionized or charged and can disassociate molecular bonds of present elements or compounds. Target materials such as GaN are placed inside the chamber and are bombarded with the ionized gas molecules. This bombardment against the target cause the atoms of the target to dislodge, with the floating atoms moving freely until collision occurs with another surface. This is called "sputter" or deposition of the target atoms on a substrate, creating a layer of atoms that increases in thickness with time, as more atoms get deposited. A substrate material, typically a wafer, is placed on the opposing end of the target material in order to allow the thin film to form [24] [48]. These depositions varied in sputtering with a mix of argon and nitrogen gasses as well as pure nitrogen gas depositions. Advances to systems such as magnetron sputtering, has drawn the attention of researchers looking for a low cost and ease of operation technique.

The use of Magnetron Sputtering reduced two problematic issues simultaneously: slow deposition rate and the extensive electron bombardment of the substrate that can cause overheating and structural damage. Magnets behind a cathode are used to trap plasma particles (free electrons) in strong electric and magnetic fields, confining the particles to the target surface.

Additionally, the magnetic field will trap the electrons in a circular path, which will significantly enhance their probability of ionizing a neutral gas molecule. The rate at which the target material is eroded will be improved, with the increase in available ions, and subsequently deposited onto the substrate [24] [48].

2.5.2 Sputtering Parameters and Material Properties

Choosing the right sputtering parameters is essential for achieving best possible film for each application, as the structural properties of the thin film strongly depend on the growth parameters (kinetics of the sputtering process and the mobility of the sputtered atoms at the surface of the substrate). Understanding of sputtering parameters is essential as they affect deposition rate, surface morphology, surface roughness, and to prevent the films from residual stress and strains which can affect structural properties. Inadequate parameters can lead to poor crystallization, and can affect deposition rate and uniformity. Additionally, they can cause damage to the target (burning, cracking or melting) and even damage the source. The parameters chosen are typically determined by the target material properties. Sputter rates will depend on throw distance, power, pressure and target size. The parameters that greatly influence this are process gas, pressure, power, substrate temperature and target to substrate distance [24].

Some examples of how sputtering parameters affect the thin film are: for achieving low surface roughness and minimum stress, a higher RF power and lower sputtering pressure is needed. There is also a close relationship between growth rate and grain size of the films. A low sputtering rate promotes the formation of small grains while a fast sputtering rate results in films with large grain size. Growth rate can be controlled by sputtering power, deposition pressure and target substrate distance. Having the ability to deposit at a lower temperature also helps to not affect sensitive substrates. Temperature affects deposition rate and although deposition can be

done without any heating, a temperature increase occurs during deposition [24]. Additional details of selected parameters are given below [24] [49] [50]:

Pressure: Pressure is highly important as it will affect whether or not plasma is created, and the energetic ion bombardment required to eject atoms. Lower pressures are typically used for best results, however significantly lower pressures can affect the surface mobility of sputtered atoms and produce poor results. At low pressures, the sputtered atoms will have higher energies than the plasma gas, fewer collisions occur on the way to the substrate and the sputtered atoms leaving the target will not scatter sideways. This will raise the percentage of atoms traveling to the substrate, causing an increase in the deposition rate. This also increases secondary electron bombardment of grounded surfaces, and the sputtered atoms will have a high surface mobility at the substrate. Additionally, the films will be denser and exhibit compressive stress. At higher sputtering pressures, the effects will be opposite. More electron collisions are encountered on the way to the substrate, resulting in the sputtered atoms being thermalized by the plasma gas. Therefore, the sputtered atoms will have a lower surface mobility at the substrate, and will be coming in at different angles resulting in the film having tensile stress.

Sputtering Power: The sputtering power also influences the rate of sputtering. There are two types of powers used, DC (for conducting targets) and RF (for poor conductors, insulators and ceramic targets) power. At low powers, the film will have tensile stress due to low surface mobility just like at high pressures. At high powers, the films have compressive stress due to high surface mobility similar to low pressures. The sputter rate will increase linearly as sputtering power is increased. Additionally, DC power will have higher sputtering rates than RF power. Applying extremely high sputtering power to achieve a high deposition rate is one of the most common errors researchers make and can lead to melting, cracking, burning of the target

material and possibly source damage. There is no clear formula for increasing deposition rates as there are many factors that can affect it. Mainly, the sputter rate will depend on the material properties of the sputtering target. The type of power used will depend on the target materials, and each one will have different power limitations due to their heat conductivity, thermal expansion properties and melting point.

Substrate Temperature and Motion: The substrate temperature will impact the properties of the deposited film. Increasing the temperature will get rid of surface contaminants at the surface of the substrate and will reduce the probability of gas incorporation such as oxygen in the film. When zero heat treatment is wanted, maintaining the substrate temperature at room temperature is important. Any heat added will come from the energetic sputtered atoms, and can influence the surface mobility of the sputtered atoms. Adding substrate rotation can increase uniformity of the grown film, and faster rotations will have more effects than slower rotations.

Working Distance: The distance between the target and substrate can affect the sputtering yield. Increasing the distance between target and substrate will lower the mobility of surface atoms at the substrate. Reducing the target to substrate distance can directly increase the deposition rate. However, being too close to the target can inversely affect uniformity. Recommended distances are 50mm to 200mm.

Gas: Argon gas will have higher sputtering rates than a reactive gas like nitrogen. Sometimes combining the use of argon and nitrogen gas or only nitrogen gas is desired for film stoichiometry. Argon gas is normally admitted near the target surface and the reactive gas will be near the substrate surface.

Targets: Highly conductive targets will allow for DC sputtering. Poor or non-conducting targets will always require RF operation, due to poor thermal conductivity. DC power will cause

burning and cracking of these targets. To minimize target damage, it is recommended that powers are slowly ramped up and down, especially when operating with RF power for poor conductive targets. Copper target backing cups are also used for maximum thermal uniformity.

CHAPTER III

METHODOLOGY

3.1 Thin Film Deposition: UHV RF Magnetron Sputtering

In this thesis, the deposition process for the growth of GaN thin films was RF magnetron sputtering, utilizing an ATC Orion Series Ultra High Vacuum (UHV) Magnetron Sputtering System from AJA International. It consists of a stainless steel vacuum chamber equipped with UVH ports. The sputter chamber can accommodate up to five UVH 2 inch targets, with confocal geometry. This allows better uniformity while depositing film, as the substrate is always in the plasma. The chamber has a sputter down configuration, with the targets positioned at the top, and the substrate at the bottom (Figure 3.1). Turbo pumping is achieved using a rotary vane type mechanical backing pump, which can achieve a base pressure of ~10^{-8}Torr. There are two power generators, direct current (DC) with a max power level of 750W and radio frequency (RF) with 300W. The substrate holder can accommodate substrates up to 4" in diameter, is equipped with controlled rotation (0-20 rpm); and radiant heating (max 850°C), with quartz halogen lamps. There are two mass controlled gas lines, argon and nitrogen. Argon gas flow uses valves to direct gas to each magnetron. For pressure control, a vacuum valve with 1000 positions between opened and closed, interfaces with Proportional-Integral-Derivative (PID) controller. A load lock chamber is used for substrate loading and to prevent contamination of the main chamber, reduce substrate load times, and waiting time to reach base pressure. In addition, a magnetic transfer arm is used to push the substrate from the load lock chamber to the main chamber [24] [48].
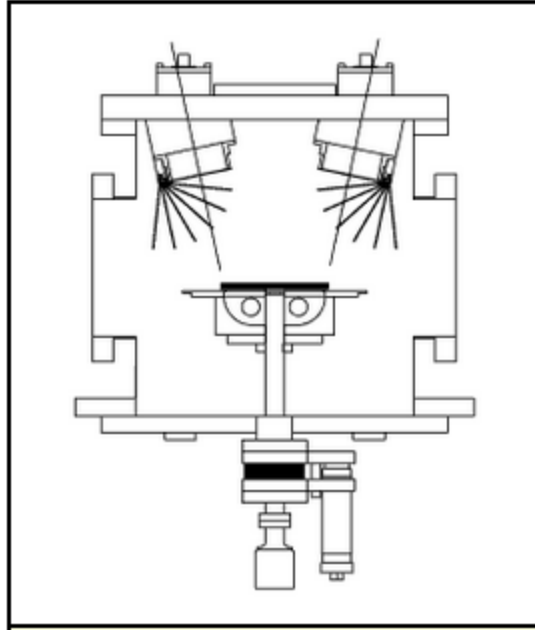
Figure 3.1 - ATC Orion 5 Sputter Down

3.2 GaN Sputtering Conditions

Choosing the appropriate sputtering conditions for the GaN target is essential, given its poor conductivity and high sensitivity to target damage. These types of targets are fragile and prone to breaking during sputter. For non-metal targets that are fragile like oxides and nitride, max power rates are lower and RF power is typically required [24] [49]. Using lower power means low deposition rates, as higher powers are known to increase the deposition times. Max power used depends on the electrical conductivity and melting point of each target material. GaN has a particularly low thermal conductivity of 2.3W/(cm*K) which limits the amount of RF power used, and previous depositions done show RF power in the 15W – 50W range for solid GaN targets [37] [38] [39] can achieve GaN thin films, as was mentioned in Chapter 2. GaN thin film have also been achieved with reactive sputtering using a Ga target [43]with DC power, than using a GaN compound target. Other research utilizes, compressed powder GaN targets, which have a higher resilience and conduction of heat, compared to solid GaN targets [44] .

31

3.3 Target and Substrate Preparation

When sputtering with new ceramic targets, it is important to slowly ramp RF power, to minimize cracking. This ramping is done both for ramping up and down to minimize the thermal shock on the target material due to intense ion bombardment. RF sputtering requires more ramping than DC sputtering, as non-conducting targets are more sensitive to thermal shock. If the operating power level is below 50W, no ramping is required. However, this varies depending on the target material and its sensitivity to thermal shock. Recommended ramping is done at 100 Watts/min for 2" targets [48]. Targets are also susceptible to target erosion patterns, which are closer to the outside of the target than DC erosion patterns. Erosion tracks on targets must be checked and target must be removed before penetration occurs. If the target has been penetrated, sputtering of the backing plate and/or cathode can occur and cause damage [48]. To achieve high quality films, the substrate should be properly cleaned prior to its insertion in the chamber and inside the chamber by applying a bias voltage to the substrate to etch it. By biasing in an operating pressure of 1-5 mTorr for 2-3 minutes, 20-30 Angstroms of surface atoms (dependent on sputter yield of material) can be removed [24].

In this research/study, a 2" GaN target with 0.125" thickness and 99.99% purity is ramped slowly (1W/s) to 50W. Presputtering was also done to remove any oxides residing at the target surface. The substrate used is a (111) silicon wafer with 500-600um thickness, (0001) sapphire wafer with 400um thickness, and glass slides. After cutting the substrates to small pieces, they were cleaned using a Kim sheet and alcohol to wipe the surface and dried using compressed air to remove any surface dust particles before loading in the chamber.

Originally, the wafers are masked using copper tape, (Figure 3.2). However, this method is inefficient as too much of the wafer is used up and the copper tape can leave impurities. To

minimize waste, the wafers are cut to smaller pieces. Because breaking the wafer in half by hand can cause it to shatter, the wafers were cut with a diamond scribe, a small scratch was made on the wafer edge on the back side of the wafer (not the polished side), then using the point of a paper clip, aligning the wafer where the scratch was made, and adding pressure. This snaps the wafer in two, allowing a clean cut, (Figure 3.3).

The samples originally contained a piece of Kapton tape in order to leave a straight edge to measure step height with the AFM. When the tape was removed, some of the film was stripped away and the measurements were found to be inaccurate. Therefore, the Sharpie method was found to be more efficient. The rest of the wafers are marked with a Sharpie X, prior to deposition. After sputtering, the mark is removed using methanol, allowing a much clearer step height measurement. This is attributed to the thinness of the Sharpie mark being closer to the thickness of the thin film than the tape.
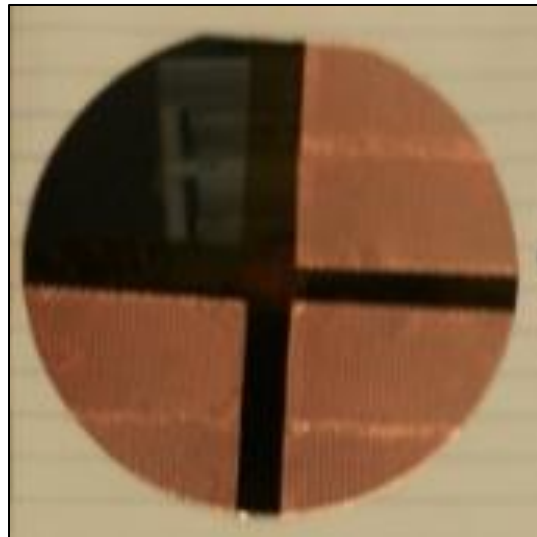
Figure 3.2 - Picture of masked silicon wafer using copper tape
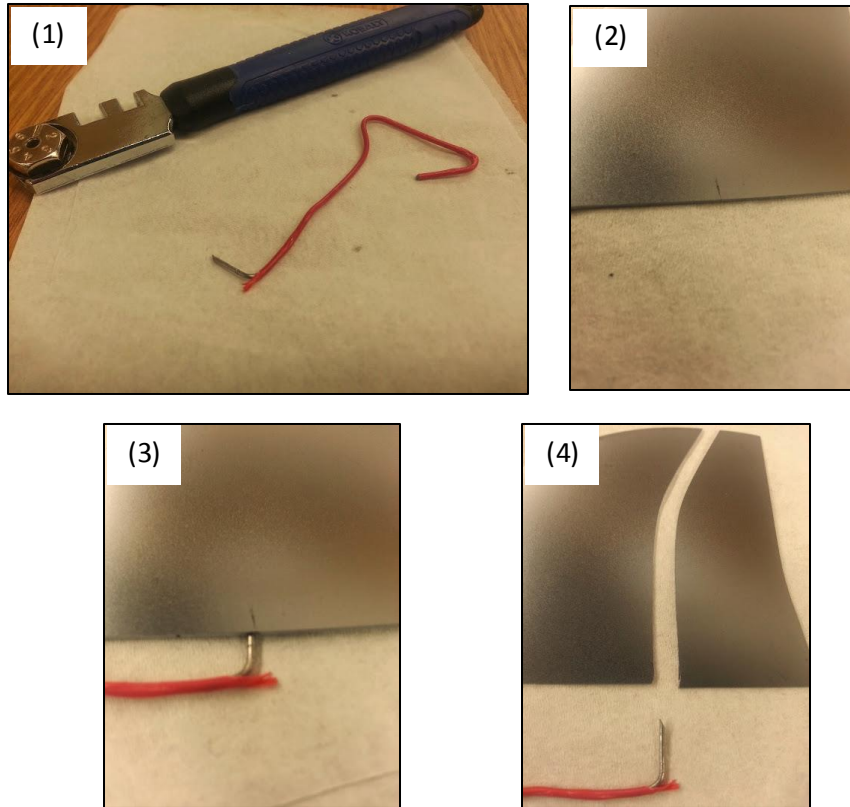
Figure 3.3 - Procedure for cutting a wafer

3.4 The Deposition Procedure

The substrates were cleaned for 5 minutes using RF bias cleaning in pure Argon gas (18 Standard Cubic Centimeters per minute (SCCM) flow). In addition, the targets were always pre-sputtered for 2-3minutes to remove any contamination and oxidation of the surface. In our process, initial experiments used 18 SCCM Ar gas flow with an operating pressure of 4-5mTorr for RF sputtering. The deposition parameters were investigated as additional information of the effects of sputtering conditions are found.

3.4.1   Preliminary Depositions: Copper, Silicon Oxide, and Silver

To gain experience using the sputtering system, initial experiments are done. A three layer deposition of Copper (Cu), Si, and silver (Ag) on an integrated circuit for verification of multiple layer deposition. The sputtering parameters are for Cu 200W RF power and 3mT pressure for 50minutes, for silicon 150W RF power and 3mT pressure for 90 minutes, and Ag 200W DC power and 3mT pressure for 40minutes. Next, a Silicon Oxide (SiO2) target is sputtered using RF power. A period of 15 minutes used for ramping up and down before the first deposition. Sputtering was done at 100W RF power at 5mT argon gas pressure. The sputtering of Si and SiO2 targets are important as they are fragile ceramic/poor conducting targets and more ramping is need the first time with this type of target. Additionally, a Cu deposition done on carbon nano fibers (CNF) to study the electrical properties of Cu coated CNFs. Using previous Cu deposition parameters to get a thickness of about 1 μm, the carbon nanofibers were coated for a period of 40 minutes on each side, at 200W DC power with 18SCCM Argon gas pressure at 3mT.

3.4.2   GaN Depositions

GaN films were deposited on silicon wafers using RF magnetron sputtering. No intentional substrate heating was used. Cooling water was circulated through the target and the chamber to prevent overheating during deposition. The chamber had a base pressure of ~10^{-7} Torr. There were three sets of experiments, initial using pure Ar gas flow, mixed Ar and N2 gas, and pure N2 gas. RF power varied from 15W to 50W. Table 3.1-3.5 shows the detail growth parameters. Initial depositions were carried out using room temperature, and post deposition temperature treatments were done after. Additional experiments were anneal during deposition at

high vacuum using the substrate heater at (700°C) to remove stresses induced in the film during the deposition.

Table 3.1 - Pure Argon gas Depositions

Sample	Base pressure (Torr)	Power (Watts)	Gas Flow (SCCM)	Pressure (mTorr)	Time (hrs.)
Si(111)/GaN	~10X-6	50	18	4	1
Si(111)/GaN	~10X-6	50	18	5	1
Si(111)/GaN	~10X-6	40	18	4	1
Si(111)/GaN	~10X-6	40	18	5	1

Table 3.2 - Mixed Argon/Nitrogen Gas Depositions

Sample	Base pressure (Torr)	Power (Watts)	Gas Flow (SCCM)	Pressure (mTorr)	Time (hrs.)
Si(111)/GaN	~10X-6	50	18:9	4	1
Si(111)/GaN	~10X-6	50	18:9	20	2
Si(111)/GaN	~10X-6	50	18:9	30	2
Si(111)/GaN	~10X-6	40	18:9	4	1
Si(111)/GaN	~10X-6	40	18:9	5	1
Si(111)/GaN	~10X-6	40	18:9	10	1
Si(111)/GaN	~10X-6	40	18:9	20	2
Si(111)/GaN	~10X-6	40	18:9	30	2

Table 3.3 - Mixed Argon/Nitrogen Gas Depositions Varied Flows

Sample	Base pressure (Torr)	Power (Watts)	Gas Flow (SCCM)	Pressure (mTorr)	Time (hrs.)
Si(111)/GaN	~10X-6	40	18:9	5	1
Si(111)/GaN	~10X-6	40	8:12	10	1
Si(111)/GaN	~10X-6	40	8:12	10	2
Si(111)/GaN	~10X-6	40	8:6	15	1
Al2O3(001)/GaN	~10X-6	40	8:6	15	1

Table 3.4 - Fixed Pressure Varied Power and Gas Depositions

Sample	Base pressure (Torr)	Power (Watts)	Gas Flow (SCCM)	Pressure (mTorr)	Time (hrs.)
Si(111)/GaN	~10X-7	40	9:6	15	2
Si(111)/GaN	~10X-7	15	9:6	15	3
Si(111)/GaN	~10X-7	40	9	15	2
Si(111)/GaN	~10X-7	15	9	15	3
Al2O3(001)/GaN	~10X-7	40	9:6	15	2
Al2O3(001)/GaN	~10X-7	15	9:6	15	3
Al2O3(001)/GaN	~10X-7	40	9	15	2
Al2O3(001)/GaN	~10X-7	15	9	15	3

Table 3.5 - Fixed Power and Pressure, Low Base Pressure Chamber

Sample	Base pressure (Torr)	Power (Watts)	Gas Flow (SCCM)	Pressure (mTorr)	Time (hrs.)
Si(111)/GaN	low ~10X-7	40	9	15	2
Al2O3(001)/GaN	low ~10X-7	40	9	15	2

3.5 Characterization Techniques

To optimize the sputtering conditions for the growth of GaN thin films, imaging tools such as the Atomic Force Microscopy (AFM) and Scanning Electron Microscopy (SEM) can be used to measure the thickness of each deposited layer, and to study surface morphology. The scanning probe microscopes permitted the observation of individual atoms and molecules to study the effects of sputtering conditions [22].

3.5.1 X-Ray Diffractometer

The X-Ray Diffractometer (XRD) is one of the most common techniques for identifying the crystal structure of solids including lattice constants and crystallography. Unknown solid materials can be identified by the orientation of single crystals, preferred orientation of polycrystalline, or amorphous if no peaks are detected. A beam of incident X-rays penetrate a

sample, and the atoms within cause the beam of X-rays to produce diffracted beams of sufficient intensities which can be measured and interpreted as the density of electrons within the crystals. For very thin film analysis, the penetration of the X-ray beam can sometimes be so high, that the thin film will not produce diffracted beams of sufficient intensity, and only the substrate diffraction patterns will dominate [22]. In this case, analyses will require long counting times, or another X-ray method called gracing incidence X-ray analysis (GIXA). In GIXA, the X-rays are incident under a very small angle to the surface of the sample, and it is very useful for analyzing very thin films [51].

A picture of the diffractometer used for the measurements described in this thesis is shown on (Figure 3.4). A list of GaN crystal orientation is also given, for hexagonal GaN (Figures 3.5) and zinc-blende GaN (Figure 3.6).

Figure 3.4 - X- Ray Diffractometer

2th	i	h	k	l
32.390	478	1	0	0
34.568	388	0	0	2
36.843	999	1	0	1
48.097	196	1	0	2
57.774	258	1	1	0
63.437	245	1	0	3
67.810	35	2	0	0
69.101	203	1	1	2
70.516	107	2	0	1
72.914	19	0	0	4
78.396	31	2	0	2
82.054	18	1	0	4

Figure 3.5 - Hexagonal GaN crystal orientation *[51]*

2th	i	h	k	l
35.604	999	1	1	1
41.345	296	2	0	0
59.901	313	2	2	0
71.666	230	3	1	1
75.390	45	2	2	2
89.829	31	4	0	0

Figure 3.6 - Cubic face GaN crystal orientation *[51]*

3.5.2   Atomic Force Microscopy

Atomic Force Microscopy (AFM) is a method used for evaluating atomic scale surface topology of thin films, by a local surface probing technique. A sharp tip is mounted at the end of a soft cantilever spring. In this method, a detection of a low power laser beam is reflected by the edge of the cantilever. The AFM can operate in various mode such as tapping, contact, or non-contact mode [22].

In this study, an AFM (Figure 3.7) with an ultra-sharp tip was used to perform the morphological studies films and roughness measurements of the grown films. AFM was operated in tapping mode.
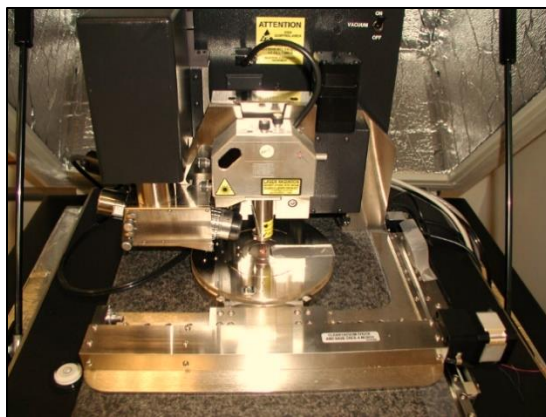
Figure 3.7 - Atomic Force Microscope

3.5.3 Scanning Electron Microscopy

Scanning electron microscopy is a standard method used for analyzing surface morphology such as grain size of the thin film. It is a type of electron microscope that produces magnified surface images by scanning a spot size (10Å in diameter) focused beam of electrons on the sample. The electrons travel at high energies and strike the target, interacting with the atoms in the sample and produce signals that can be used to obtain information such as surface topography and composition. For best results, samples should be electrically conductive, and scanned at low vacuum. For non-conductive samples, a charge build up is observed when scanned by the electron beam [22]. To reduce this, sample preparation must be done by either coating it with electrically conducting material or applying electrically conductive paste such as graphite to increase conductivity and ground the sample (Figure 3.8).

Figure 3.8 - Samples prepared with copper grid and graphite paste

3.5.4   Energy-dispersive X-ray spectroscopy

Energy-dispersive X-ray spectroscopy (EDS) is interfaced with SEMs, and is used as an analytical instrument to detect elemental composition of a sample. Similar to the operation of SEM, an emission of beam of electrons is focused on the sample, exciting the outer electrons of an atom, and thus, generating energy. The amount of energy emitted can be characterized for specific elements. Each element has a unique atomic structure giving it a set of unique peaks on its X-ray emission spectrum. Where the electron beam serves to excite characteristic x-rays from the probed area of the specimen. The operating voltage is normally 10kV. For the samples that are less than 100nm it was best to set a lower operating voltage of 5kV.

3.5.5   X-ray photoelectron spectroscopy XPS

X-ray photoelectron spectroscopy (XPS) is used for the chemical characterization of thin films. This is a true form of surface analysis since the detected electrons and ions are emitted from surface layers less than ~15Å deep. A depth profile can then be made by sputter etching the

film and analyzing the exposed surface. It is typically able to detect all the elements in the periodic table. [52] Figures 3.9 and 3.10 give references for the binging energies of different chemical states of Ga.
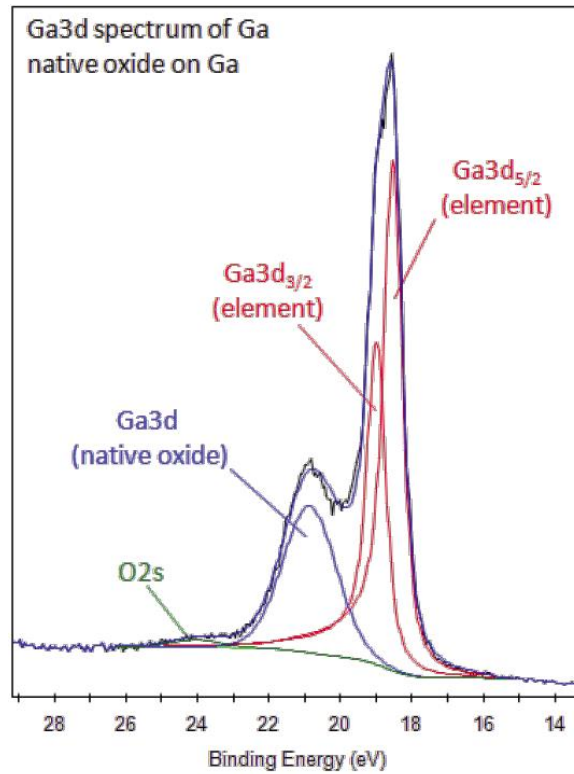
Figure 3.9 - XPS Reference of Ga binding energy *[52]*

Chemical state	Binding energy Ga2p$_{3/2}$ / eV	Binding energy Ga3d$_{5/2}$ / eV
Ga elemental	1116.7	18.7
GaAs	1116.9	19.1
Ga2O3	1118.0	20.5
GaAs native oxide	1117.8	20.3
Ga native oxide	1118.7	20.9

Figure 3.10 - Ga binding energies at different chemical states *[52]*

3.6 Generating a Deposition Sequence (Recipe)

Sputtering can be done manually or automatically by generating a recipe. The manual option is normally used when there are problems running a process, however, running a process simplifies the depositions, as they can easily be selected to run the same process again. Additionally, in the manual mode, the time for each process has to be monitored carefully, while the automatic process begin and stop on their own. To create a recipe, at least four deposition layers are needed. The first two layers required are used for bias cleaning. Bias cleaning is done using RF power to first strike a plasma, and secondly to clean the surface of the target. The first layer is the striking layer done at 50W RF power and 30mT pressure (a high pressure is needed to strike a plasma) using pure Argon gas. The second layer is the surface bias clean with sputtering parameters of 50W RF power and the pressure can now be lowered to 3mT pressure (if required). As mentioned in previously, two-three minutes of bias cleaning can remove twenty – thirty Angstroms of surface atoms, when sputtering within (1-5 mTorr). The last two layers are target strike and the coating layer. Target striking is used to strike a plasma at the target using a low power (50W) and high pressure (30mT). In this layer the time can be increased for a desired amount to clean the surface of the target (new targets can contain oxide layers). In the coating layer, the pressure can then be lowered if required and the RF or DC power can be increased. If additional deposition layers they can be created and added in the sequence. Once each separate layer is created and verified, a process can be created, and the process can be ran. Once the process is running, processing screen will appear showing all the various parameters indicating the current process is on (Figure 3.10). It is important to monitor the screen to make sure the parameters set are correct, as well as making sure plasma is created (indicated by the pink color, if there is no plasma the color is grey).
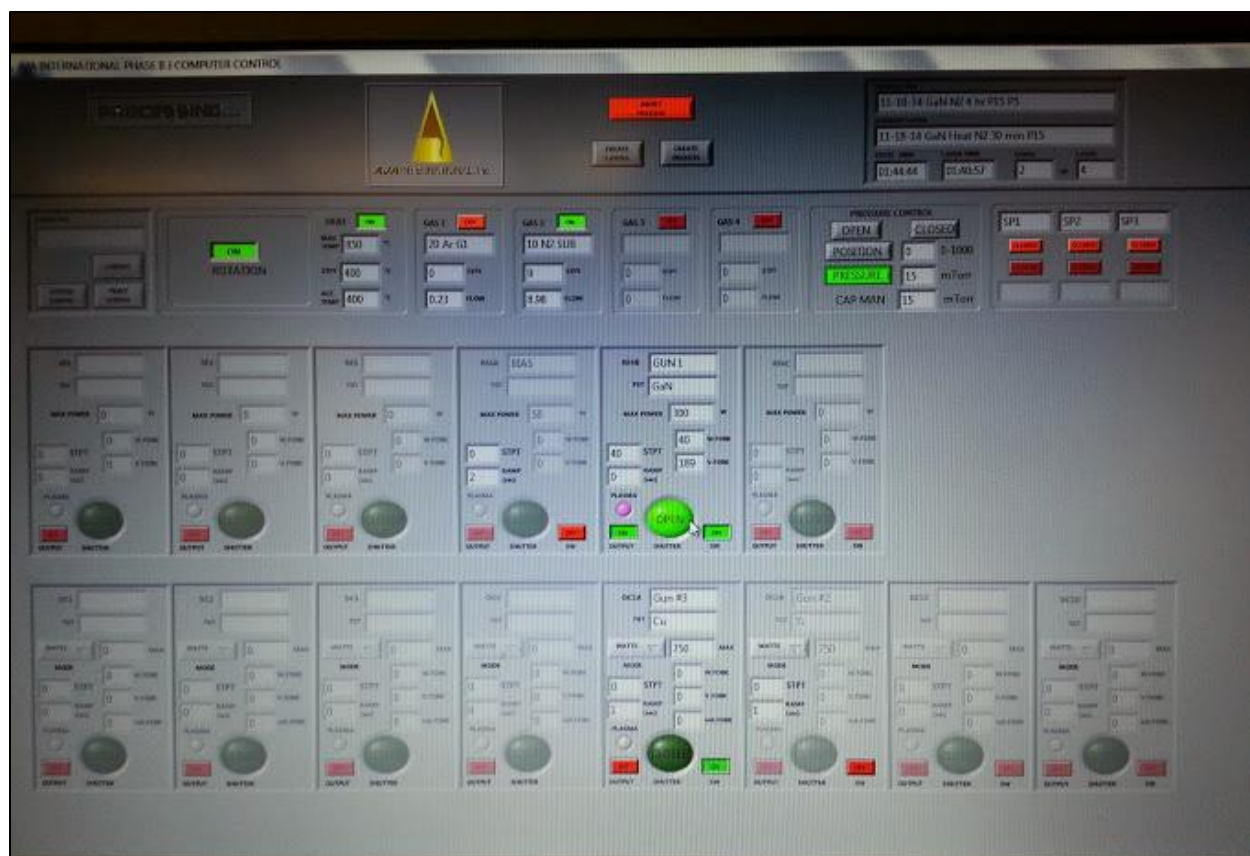
Figure 3.11 - Processing screen

44

CHAPTER IV

PRELIMINARY RESULTS

4.1 Copper Deposition

The sputtering of copper, silver, and silicon thin films on integrated circuit wafers gave an understanding for sputtering conditions. The copper sputtering rate is used for comparison to other material sputtering rates. Figure 4.1 is a picture of the resulting depositions of copper, silicon and silver (in that order). The silver color is the thin film while the darker area is the integrated circuit without thin film. A SEM surface image taken shows the formation of silver grains of different sizes (Figure 4.2). This indicates that polycrystalline thin film has grown. Figure 4.3 is a surface image of the border between the deposited film and the uncovered IC wafer. A final SEM cross-sectional image shows each deposited layer. The substrate, then the copper, then silicon and finally the silver. Silver's sputtering rate is 2.2 relative to 1 of copper, as shown in Figure 4.5, indicating if 1 µm is grown for copper for 1 hour, silver's thickness will be approximately 2.2 µm. The final layer of silver is about 2.4µm. The next layer is a mix of the copper layer and the silicon layer. Silicon's sputter rate is 0.38 that of copper, this is too small to be able to differentiate between the two layers. It can be assume that copper grew to a little over 1 µm and the rest is silicon. This experiment did provide comparable results of the silver and silicon materials sputter rates relative to copper.
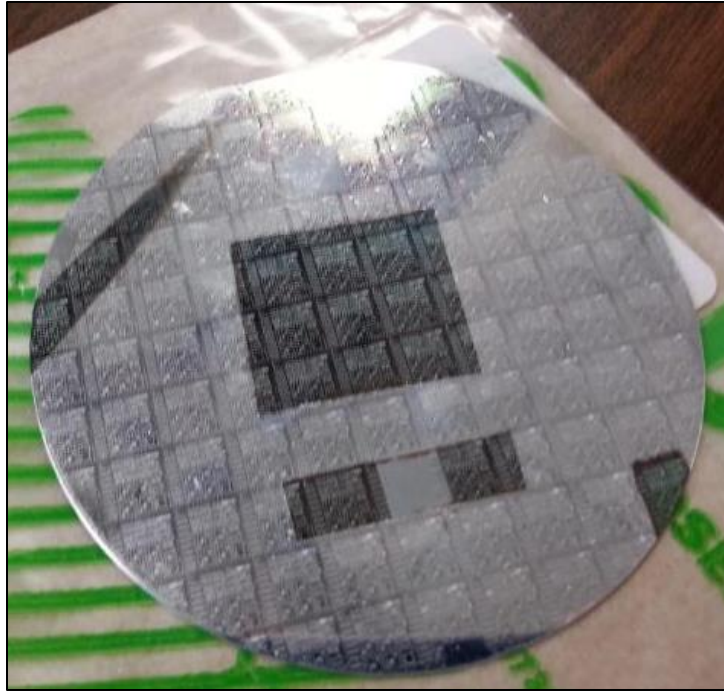
Figure 4.1 - Picture of deposited film on IC wafer

| 200 nm | EHT = 5.00 kV | Signal A = InLens | Date :17 Apr 2014 |
| | WD = 7.7 mm | Mag = 1235.16 K X | Sample ID = |
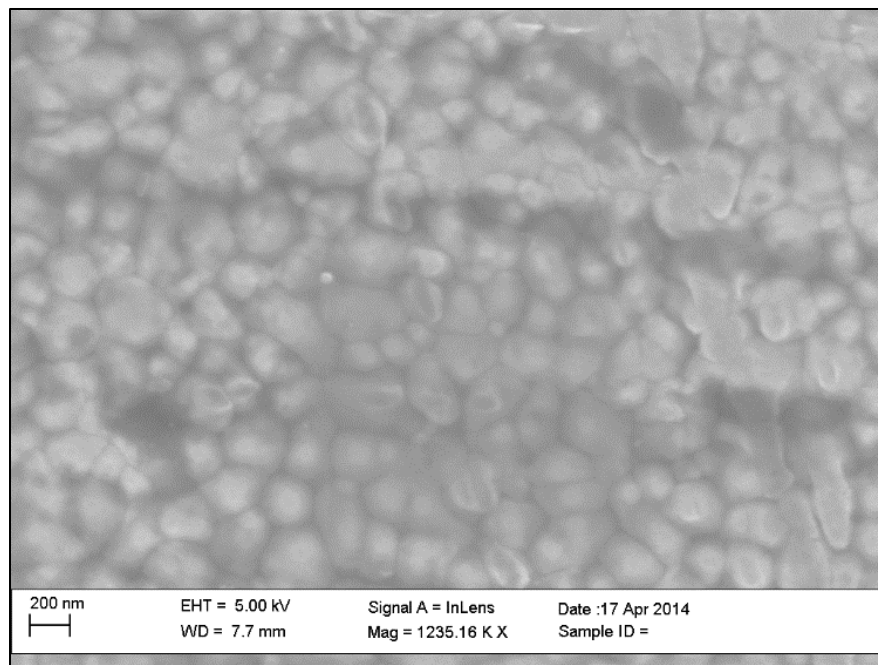
Figure 4.2 - SEM surface image showing grain formation
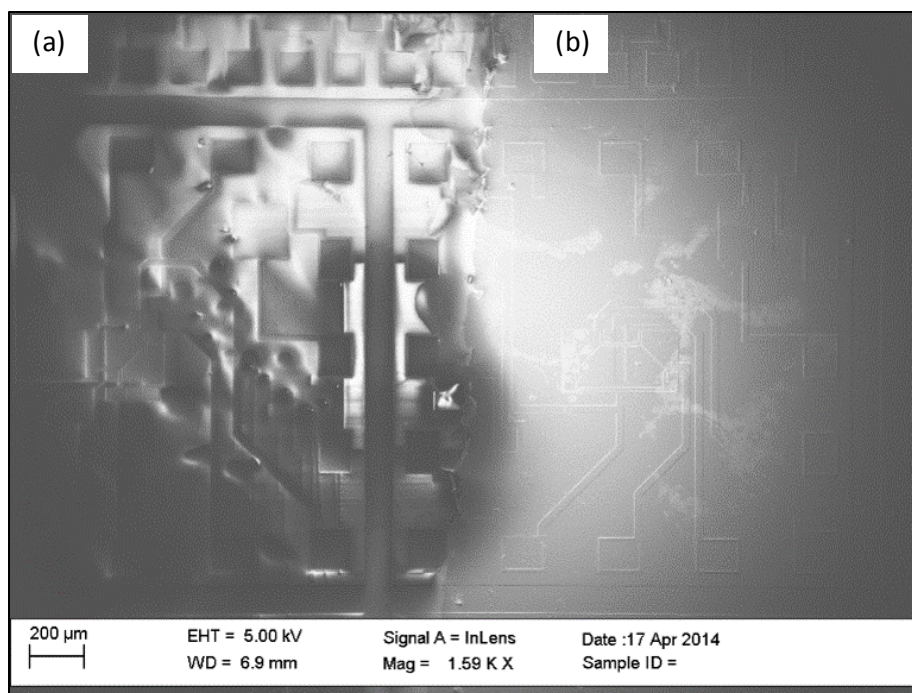
Figure 4.3 - SEM surface image: division of (a) uncovered IC wafer and (b) deposition
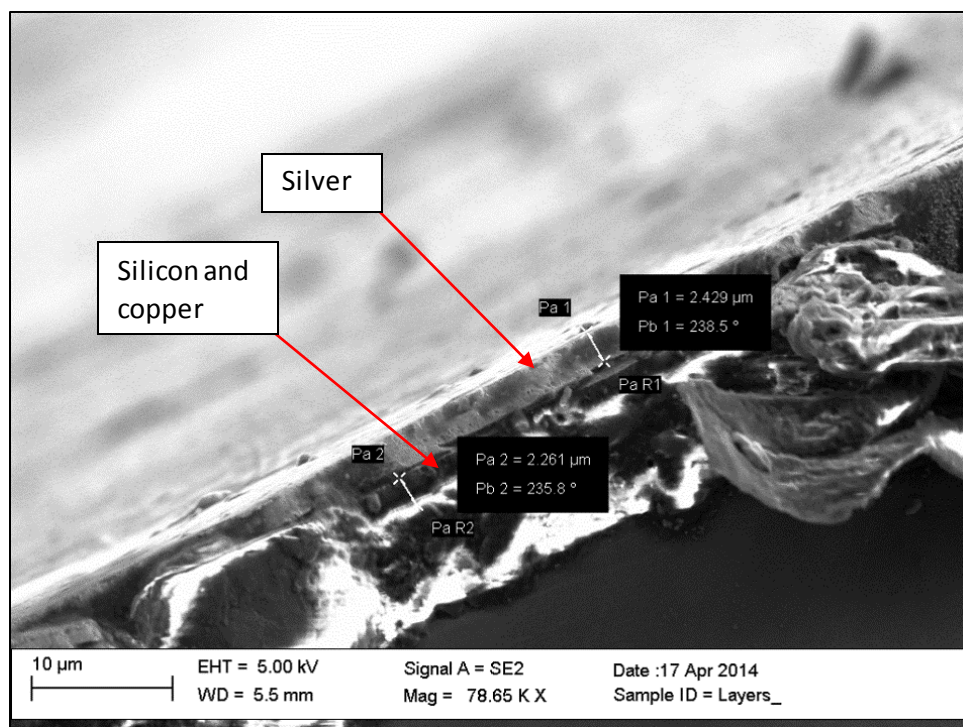
Figure 4.4 - SEM cross sectional image showing each deposited layer

Al	0.77	Ge	1.10	Sb	3.96
Al2O3	0.16	Ir	0.66	Si	0.38
Ag	2.24	Mo	0.51	SiC	0.39
Au	1.90	Mn	1.07	SiO2	0.49
Be	0.19	Nb	0.48	Sm	1.21
Bi	1.76	Ni	0.70	Su	1.41
C	0.05	Os	0.54	Ta	0.46
Co	0.62	Pb	3.76	Th	0.90
Cr	0.65	Pd	1.41	Ti	0.41
Cu	1.00	Pt	0.97	U	0.81
Dy	1.27	Rb	4.89	V	0.41
Er	1.08	Re	0.57	W	0.42
Fe	0.52	Rh	0.97	Y	1.023
GaAs	1.83	Ru	0.71	Zr	0.70

Figure 4.5 - Sputter yield rates relative to copper *[24]*

The copper deposition grown using parameters of 200W DC power, 3mT pressure and 18SCCM Argon gas achieved 1 μm of copper for 40minutes. This verified that 1 hour of copper achieves a little over 1μm. Using this knowledge, copper depositions on CNFs are grown to 1 μm on each side. The Cu deposition was in assistance to another professor working on electrical properties of Cu coated nanofibers. Figure 4.6 shows the before and after picture of the CNFs. After a 40 minute deposition, the carbon nanofibers looked like pennies and a 1 μm deposition on each side was verified by the electrical properties exhibit on the CNFs.
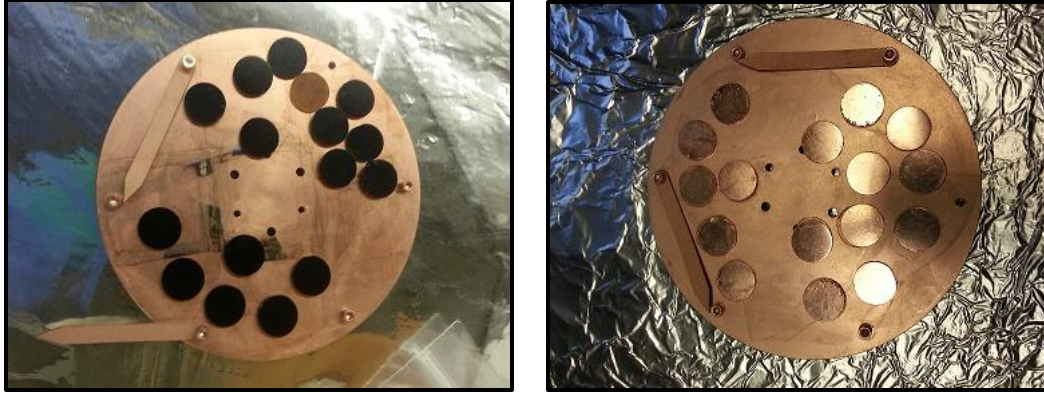
<div align="center">(a)   (b)</div>

Figure 4.6 - Nanofibers before (a) and after (b) Cu coat

The final deposition is done using a SiO2 target in order to sputter using RF power resulted in a film thickness of about 180nm. This experiment was important as it was the first fragile ceramic type target used. More ramping is needed when a new target is used. A period of 15 minutes is done for ramping up and down before the first deposition. Sputtering was done at 100W RF power at 5mT argon gas pressure.

These preliminary experiments are helpful to gain experience using the sputtering system. It also served for verification of the system, as the sputter yield rates of the materials are compatible to that of the sputter yield rates provided by AJA International. Additionally, the grain formation of the silver thin film signifies that polycrystalline film can be grown.

CHAPTER V

GAN EXPERIMENTS: RESULTS AND ANALYSIS

The characteristics of the thin films strongly depended on the sputtering gas, RF power, pressure and temperature. Polycrystalline GaN is grown under the sputtering conditions of 40W RF power, 5mT working pressure, using pure nitrogen gas with a substrate temperature of 700C. A 60% nitrogen or higher is needed to increase the nitrogen incorporation in the thin film and achieve stoichiometry. Otherwise, the argon ions have enough energy to resputter at the surface of the thin film, leaving them nitrogen deficient. Additionally, target poisoning is observed when sputtering with a higher percentage of argon to nitrogen. Sputtering with a higher percentage of argon gas required higher pressures of 20mT to 30mT to suppress the resputtering at the surface of the thin film or target surface.

5.1 Argon Depositions

Sputtering with pure argon gas resulted in the thin films being highly nitrogen deficient, with an average N/Ga ratio of 0.16, regardless of the power or pressure. Tables 5.1 lists the characteristics for the films deposited using pure Ar. EDS spectra indicated the films contained Ga, N, with impurities of C and O. The thickness of the film had a linear relation with increasing RF power, with an increase of approximately 20 nm observed as the power is raised by 10W. The fastest deposition rate is achieved using the highest power and the lowest pressure (50W, 4mT) and the slowest deposition rate with the lowest power and highest pressure (40W, 5mT) which correlates with known sputtering conditions for achieving a fast deposition rate [24]. An

inspection of the GaN target's surface revealed a black layer of material. This phenomenon (target poisoning) is observed to be dependent on the sputtering gas and pressure used. More on target poisoning will be discussed in section 5.7.

Table 5.1 – Characteristics of RF power using pure Argon gas (a) 4mT and (b) 5mT

4mT						
Power (W)	Thickness (nm)	Ga %	N %	O %	N/Ga Ratio	Time (hr.)
40	175	30.11	4.87	26.22	0.16	1
50	198	38.63	6.19	28.45	0.16	1

(a)

5mT						
Power (W)	Thickness (nm)	Ga %	N %	O %	N/Ga Ratio	Time (hr.)
40W	165	28.25	5.48	22.04	0.19	1
50W	185	30.97	4.05	33.09	0.13	1

(b)

The color of the films varied from light blue to dark blue for 50W RF power, and dark yellow to black (Figure 5.1). As reported by [44], dark color films are attributed to gallium atoms forming clusters. The color of the film is blue when a higher concentration of oxygen is in the film, which is attributed to gallium oxide. Additionally, when analyzing the films using XPS, binding energies for the film deposited at 40W 5mT, the binding energies of Ga3d have two peaks (20.4eV, 18.8eV) Figure 5.2 (a). Elemental gallium has a biding energy at 18.5eV, this indicates the film contains the presence of elemental gallium. GaN has a binding energy of 19.8 eV, the positive shift peak at 20.4 eV contains both GaN and Ga2O3 (20.5eV). Figure 5.2 (b) is the nitrogen binding energy spectrum, N1s (~397eV) is seen, the additional peaks from (396-393eV) are from Ga satellites. The data from XPS reveals that carbon component are seen only at the surface, as no carbon is detected after surface etching, Figure 5.3 (a). (For all other films in

51

this thesis, the carbon elements are seen only at the surface and not incorporated within the thin film). Oxygen is observed even after surface argon etching, indicating oxygen incorporation during the thin film deposition (Figure 5.3 (b)). Oxygen impurities can be coming from the sputtering gasses (they are not high purity gasses), from residual impurities from the vacuum chamber due to poor vacuum, or from compressed air used to keep the base pressure valve opened. SEM surface images revealed the presence of small grains of various sizes formations, which are not very define, Figure 5.4. This means the film is polycrystalline close to amorphous.
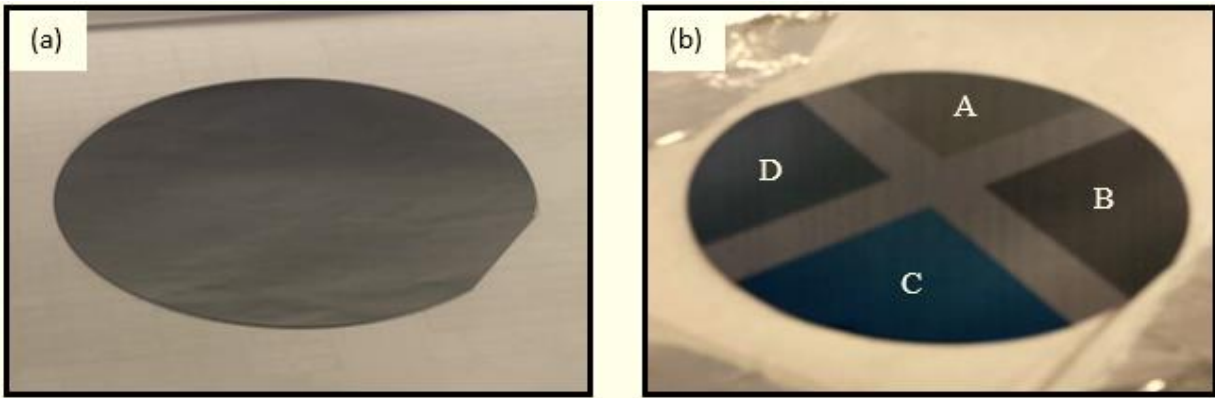
Figure 5.1 - (a) silicon wafer, (b) GaN depositions: A-40W 4mT, B 40W 5mT, D 50W 4mT, C 50W 5mT
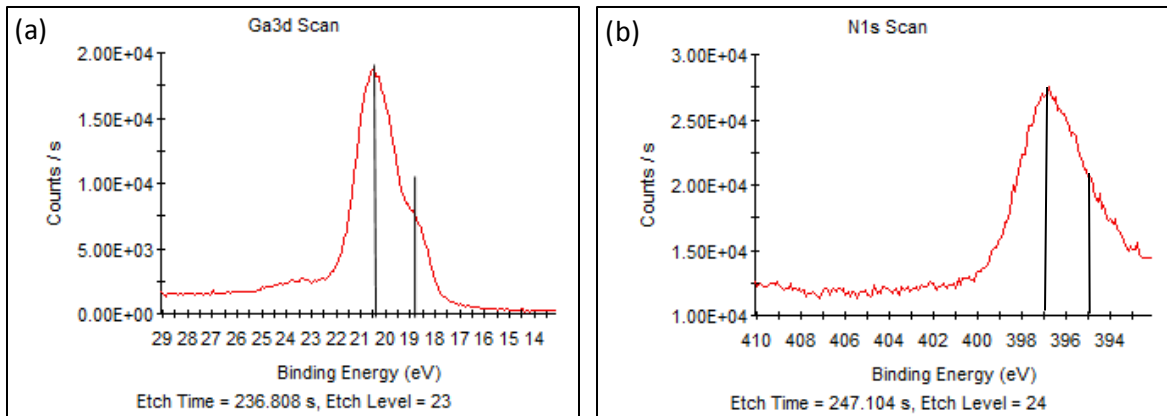
Figure 5.2 - XPS spectra of (a) Ga 3d and (b) N1s binding energy (eV)
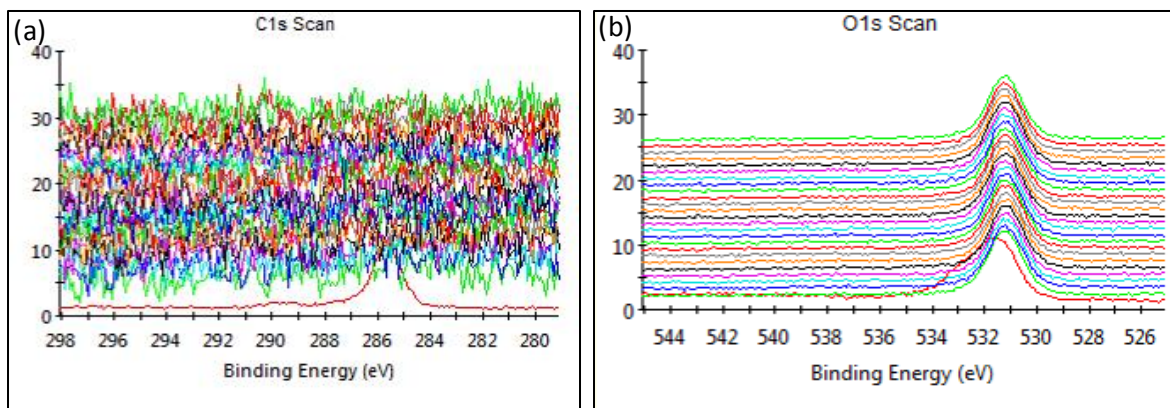
Figure 5.3 - XPS: depth profile of (a) Ga, (b) N, (c) C, and (d) O
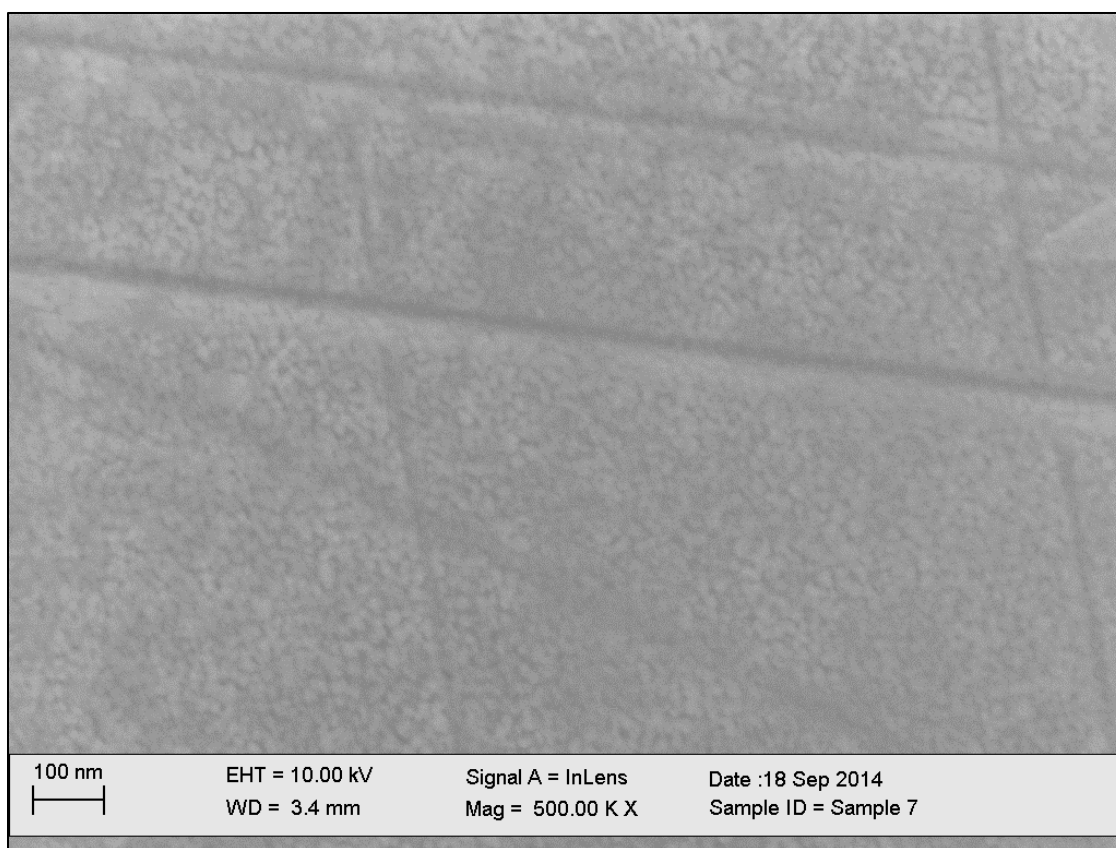
Figure 5.4 - SEM surface image of 50W 5mT pure argon

5.2 Depositions Using Argon and Nitrogen Mixed Gas

Nitrogen gas (N2) is introduced as a sputtering gas along with argon gas, with 30% nitrogen concentration. Table 5.2 depicts the characteristics of the depositions of GaN made with 40W RF power and varied pressures. With the inclusion of N2, the N/Ga ratio increased but was still below stoichiometry. It can also be observed that the atomic percentage of nitrogen is increased with increased pressure. Table 5.3, lists the characteristics of the GaN film prepared at 50W RF power and varied pressures. An increase of nitrogen concentration with increasing pressure was once again observed. Comparing the N/Ga from 40W to 50W, the N/Ga ratio was lower at 50W, indicating that RF power may have been too high, and the ion bombardment produces a film more deficient in nitrogen. The deposition time for pressures of 20mT and 30mT has to be increased to 2 hours, as the deposition rate is slower at higher pressure. SEM surface images of 40W RF power and pressure of 5mT (Figure 5.5) and 20mT (5.6) are slightly more defined than when sputtering with pure Argon gas. The grain sizes vary in size confirming the films are polycrystalline, with the grains ranging from 15nm to 21nm. The increase pressure did not affect the grain size. However, the films still appeared to have some smooth areas with no clear grain boundary, revealing a polycrystalline to amorphous structure.

Table 5.2 - Depositions at 40W RF power and varied pressure

Sample	Thickness (nm)	Ga %	N %	O %	N/Ga Ratio	Time (hrs.)
40W 5mT	74.357	21	4.49	30.84	.213	1
40W 5mT	146.43	13.725	3.635	25.575	0.28	2
40W 20mT	29.63	7.395	2.13	14.05	0.28	2
40W 30mT	16.9	3.455	1.63	7.88	0.47	2

Table 5.3 - Depositions at 50W RF power and varied pressure

Sample	Thickness (nm)	Ga %	N %	O %	N/Ga Ratio	Time (hrs.)
50W 20mT	37.58	10.35	2.32	18.95	0.22	2
50W 30mT	18.1	5.25	1.86	10.79	0.35	2

100 nm

EHT = 10.00 kV
WD = 4.2 mm

Signal A = InLens
Mag = 500.00 K X

Date :26 Nov 2014
Sample ID = 40 W 10 mTorr ArN Si
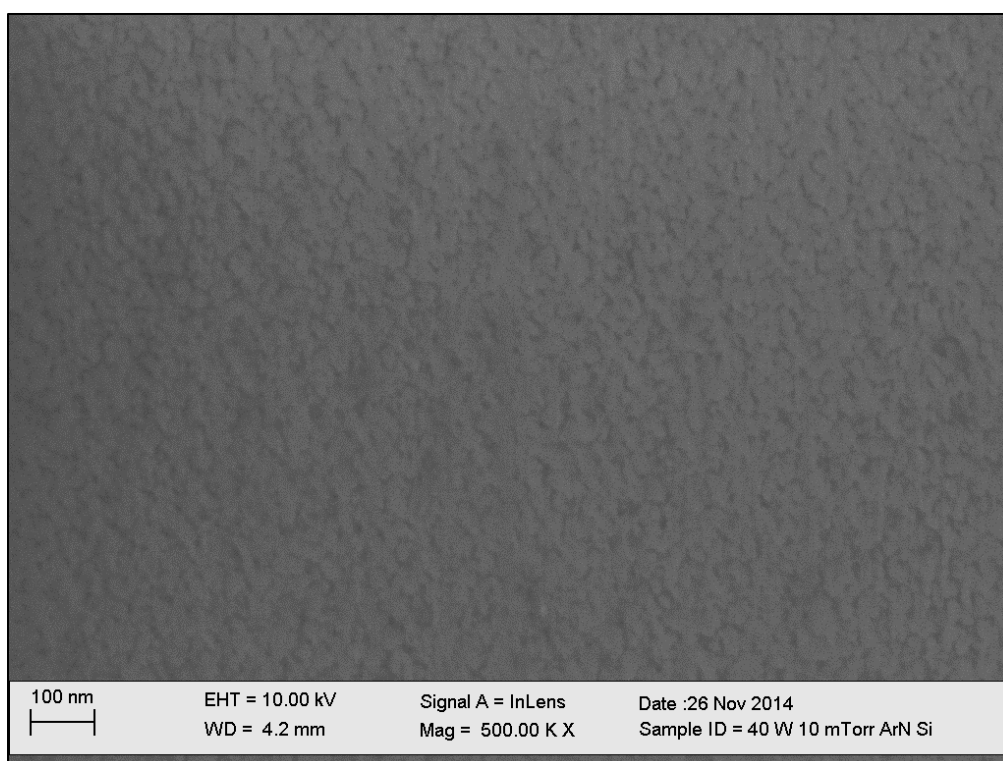
Figure 5.5 - 40W 5mT Ar/N2 18:9 15nm 21nm

100 nm   EHT = 10.00 kV   Signal A = InLens   Date :26 Nov 2014

WD = 3.4 mm   Mag = 500.00 K X   Sample ID = 40 W 20 mTorr ArN 8/12 2 hrs
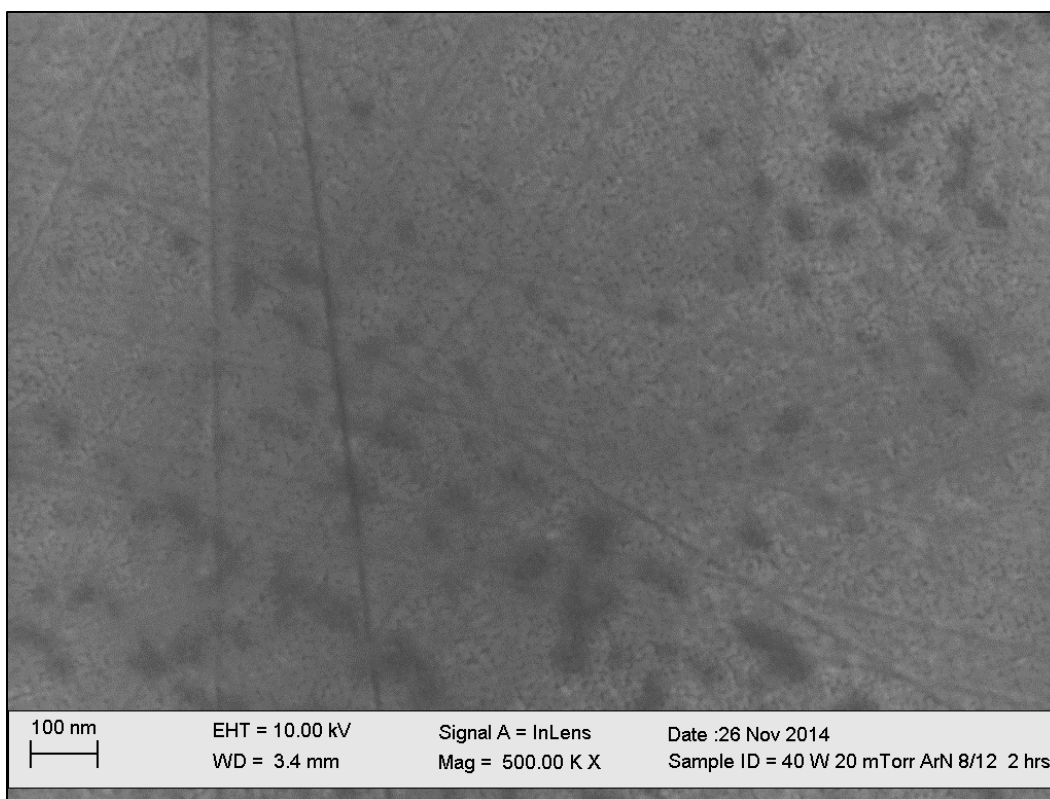
Figure 5.6 - 40W 20mT Ar/N2 18:9 grain size (15nm 21nm)

At this point, a visual inspection of the target was done to check for target poisoning. It was observed that the introduction of N2 reduced target poisoning, but the black surface layer was not completely reduced. Table 5.4 lists the characteristics for depositions made after the target had been "cleaned" following depositions at higher pressures using nitrogen gas. After a deposition done at 50W RF power and 4mT, the nitrogen concentration has increased compared to sputtering in pure argon gas, however the black surface material has increased. When sputtering in 40W RF, the effect of target poisoning is not as high, however the target does not start to get "cleaned" until a pressure of 10mT. A final deposition is made after sputtering at 10mT 40W, indicates that sputtering at 40W 5mT had increased nitrogen concentration. This indicated that the target poisoning has a major effect on the stoichiometry of the GaN films. SEM surface image taken from selected film showed the grain formation. Figure 5.7 shows the

SEM surface image from deposition done using 10mT pressure with an average of 14nm grain size. The deposition done after the target is cleaned with 5mT had an increase in N/Ga and also had larger grains (Figure 5.8).

Table 5.4 - Characteristics of depositions to test the effects of target poisoning

Sample	Thickness (nm)	Ga %	N %	O %	N/Ga Ratio	Time (hrs.)
50W 4mT	99.539	33.7	11.08	34.07	.33	1
40W 4mT	78	6.42	1.15	14.62	.18	1
40W 5mT	72.67	14.6	4.1	23.8	.28	1
40W 10mT	41	11.4	4.62	20.21	.40	1
40W 10mT	43	11.9	5.03	20.41	.42	1
40W 5mT	41.19	25.4	14.41	26.58	.56	2

200 nm	EHT = 10.00 kV	Signal A = InLens	Date :26 Nov 2014
	WD = 3.7 mm	Mag = 500.00 K X	Sample ID = 40 W 10 mTorr ArN Si
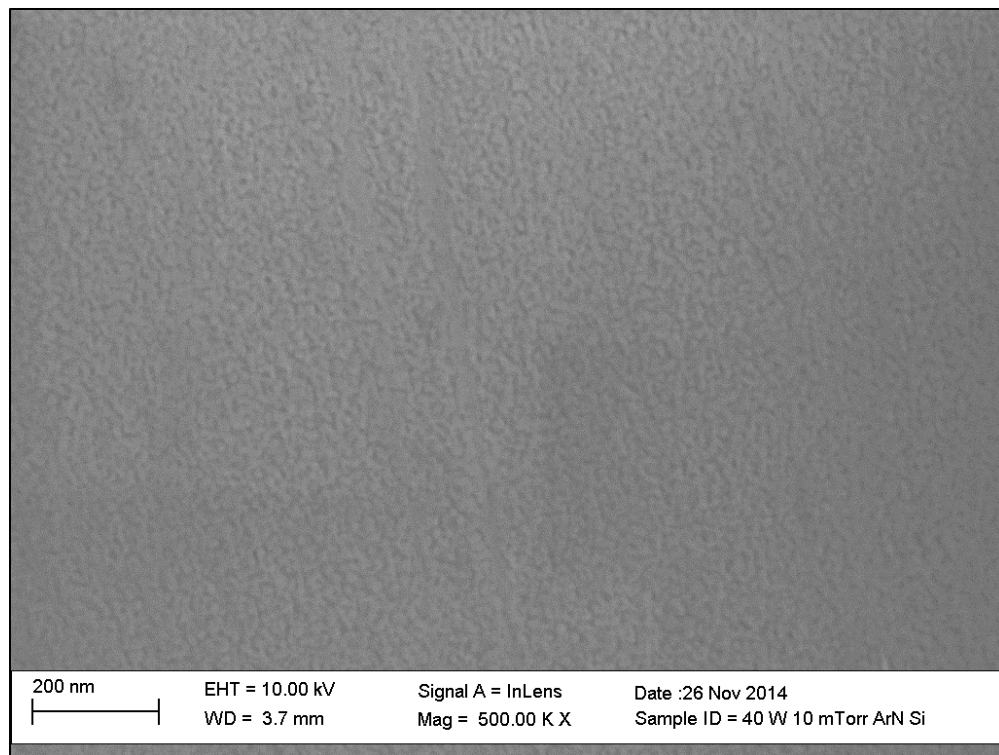
Figure 5.7 - 40W 10mT 40% N2 1hrs 12nm 16nm
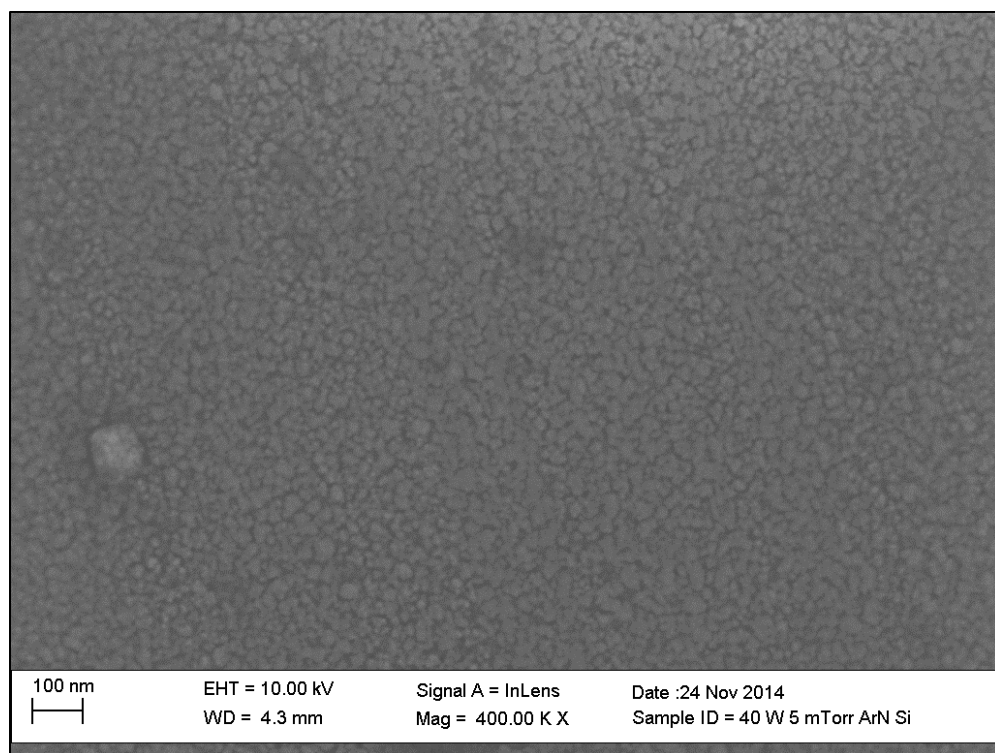
Figure 5.8 - 40W 5mT 30% N2, grain size (25.86nm to 34.59nm)

5.3 Depositions at Various Concentrations of Nitrogen Gas

Table 5.5 lists the characteristics for GaN films sputtered at various N2 ratios and varied pressures. It indicates that the films became close to stoichiometric in a pure N2 gas with high pressure. Sputtering in pure Argon gas resulted in nitrogen deficient films. With the absence of N, O impurities at higher power make the films Ga2O3. As N concentration was increased, the films began to look more yellow (GaN color). The films sputtered at 30% and 40% nitrogen begasn to have an increase in N atomic percentage. Eventually the films became amorphous and turned black. It was observed that the inclusion of N gas as the sputtering gas enhances the N incorporation in the films. This is further investigated by increasing the N flow rate from 0% to 100%. Depositions made at 60% N2 gas or at pure N2 gas with varied powers of 40W to 15W showed that the N percentage increases in the films significantly. At low powers, N atomic

percentage surpasses Ga. Further experiments could be done for optimized power rating, however in this study, for the purpose of finding optimized sputtering conditions with a decent deposition rate, the operating power was kept at 40W. Poisoning of the target was also observed when Argon flow rate was higher than N. Sputtering at higher pressures of 20 and 30mT did not affect the surface of the target.

Table 5.5 - Depositions at various N2 flow rates and varied pressures

40W							
Nitrogen Gas (%)	Pressure (mT)	Thickness (nm)	Atomic percentage			N/Ga Ratio	Time (hrs.)
			Ga (%)	N (%)	O (%)		
0	5	175.63	28.3	5.48	22.04	0.19	1
25	5	74.3	21.035	4.49	30.84	0.21	1
33	5	146.43	13.7	3.635	25.58	0.27	2
33	10	146	35.02	7.2	45.47	0.21	2
40	10	35.45	8.69	2.85	16.41	0.33	1
40	10	64.72	8.62	3.22	17.31	0.37	2
60	15	15.42	6.98	3.51	14.89	0.5	1
60	15	34.05	8.48	3.44	16.07	0.41	2
100	15	22.22	4.07	2.99	8.89	0.73	2

Sputtering at pure Argon gas, the thin films are nitrogen deficient with a polycrystalline to amorphous structure. Although the film showed a peak at 36.7°, related to wurtzite structure, eventually the film became amorphous due to the intense ion bombardment of the argon ions, as can be seen in Figure 5.9. In Figure 5.9 (c), the two hour deposition begins to take an amorphous structure. This same effect was seen in [44], explained as a resputtering at the substrate and leaving it nitrogen deficient from the intense ion bombardment of the argon ions. As the nitrogen concentration is increased, a stronger peak began to form at 36.7°. At low pressures the films have a cubic structure, as the pressure is increased, a stronger peak at 36.7° becomes more dominant. SEM surface images showed small grains for the films (Figures 5.10 and 5.11).
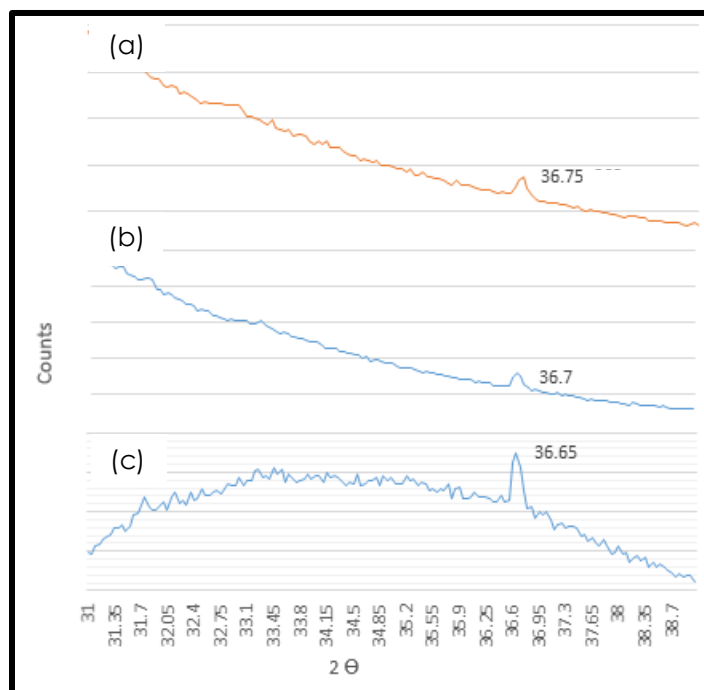
Figure 5.9 - 40W 10mT (a) 33%N2 1hr, (b) 40% N2 1hr, and (c) 40% N2 2hrs.
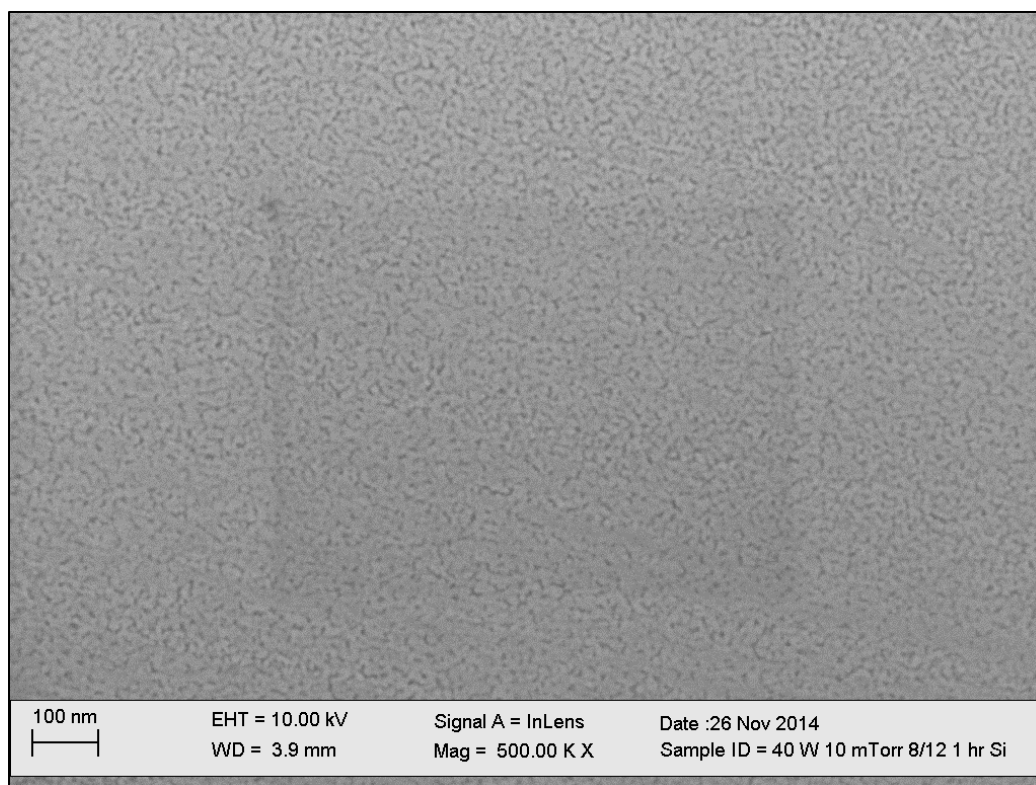
Figure 5.10 - 1hr 40W 10mT (8:12) grain size (26.14nm to 19.60nm)
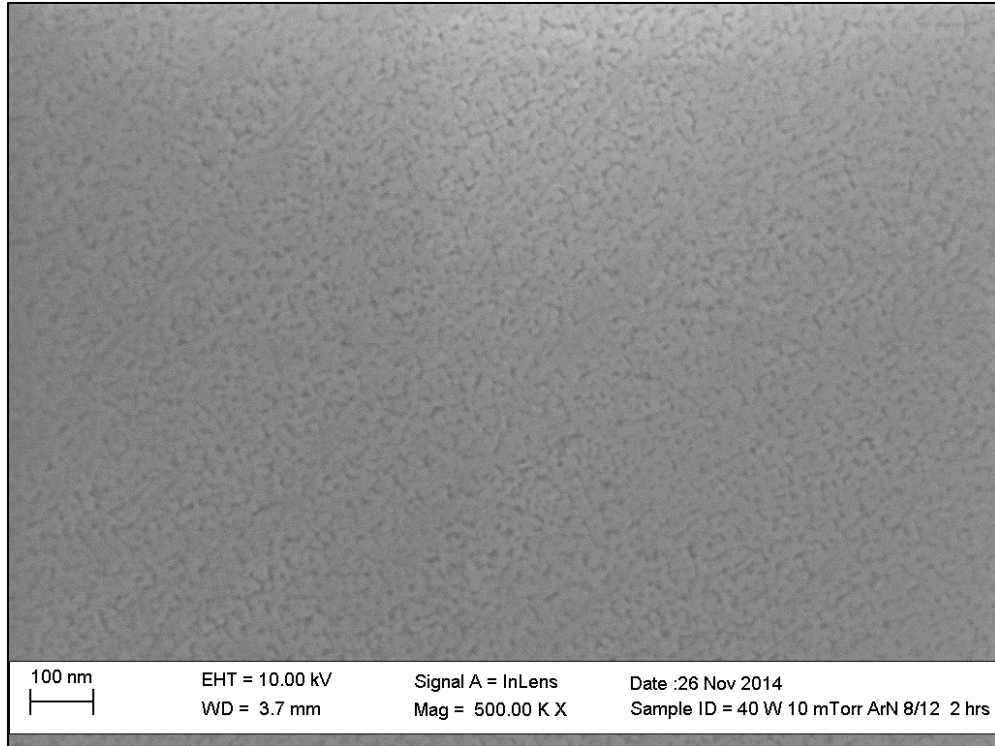
Figure 5.11 - 2hr 40W 10mT (8:12) (25.78nm, 22nm)

5.4 60% N2 or pure N2 depositions

A sputtering pressure of 15mT was chosen as an optimized pressure so the pressure does not to cause the resputtering effect at the substrate or the target surface. The RF power was also varied at either 40W or 15W to investigate the effect on powers. Additionally, a sapphire wafer was used as a substrate. Sapphire's better lattice match to GaN should positively affect the GaN growth. The deposition times are 2 hours at 40W RF power and 3hrs at 15W RF power, as the deposition rate was expected to be much slower at these conditions. Figure 5.12 depicts the effect of gas types and powers on the deposition rates. As mentioned, sputtering at higher or pure N2 has slower deposition rates.
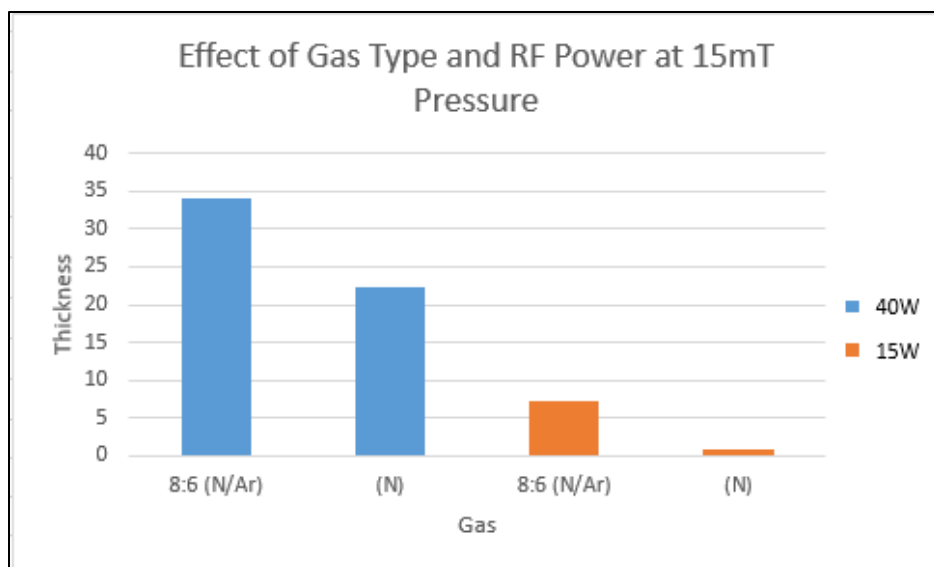
Figure 5.12 - Fixed 15mT pressure depositions with varied power and gas type

Table 5.6 and 5.7 show the N/Ga ratios of sputtering at 15mT pressure with varying parameters of power, gas type, and substrate type. At 40W RF power with pure N2 greatly increased the N/Ga ratio. The N atoms of the N2 gas enhanced the incorporation of N in the GaN thin film. The sapphire wafer also increased N content on all four depositions. Sputtering using an Ar/N2 mix yielded larger grains which is due to the argon ion bombardment (Figure 5.13). Sputtering using pure N2 had slightly smaller grains (Figure 5.14). At 15W RF power, both gas types had increased N contents, with the N content being even higher than gallium. However, due to the deposition time being only three hours, the thin film was only a few nanometers thick, and the SEM surface image reveal amorphous film, as there are no grain formations (Figure 5.15). If they had been grown thicker, it might have given it time to form.

62

Table 5.6 - Characteristics of films using 15mT pressure with varying parameters of power, gas type and substrate type on Silicon wafer

15mT on Silicon Wafer							
Nitrogen Gas (%)	Power (W)	Thickness (nm)	Atomic percentage			N/Ga Ratio	Time (hrs.)
			Ga (%)	N (%)	O (%)		
60	40	34.0575	7.7	3.51	14.89	.455	2
60	15	7.3255	2.69	2.155	6.213	.801	3
100	40	22.225	4.33	3.71	9.34	.856	2
100	15	3.1	1.15	2.88	5.84	2.5	3

Table 5.7 - Characteristics of films using 15mT pressure with varying parameters of power, gas type and substrate type on Sapphire wafer

15mT on Sapphire Wafer							
Nitrogen Gas (%)	Power (W)	Thickness (nm)	Atomic percentage			N/Ga Ratio	Time (hrs.)
			Ga (%)	N (%)	O (%)		
60	40	32	5.5	6.26	57.99	1.1	2
60	15	6	1.92	3.37	56.14	1.75	3
100	40	22	5.5	6.26	57.99	1.13	2
100	15	3	3.13	3.3	55.835	1.05	3
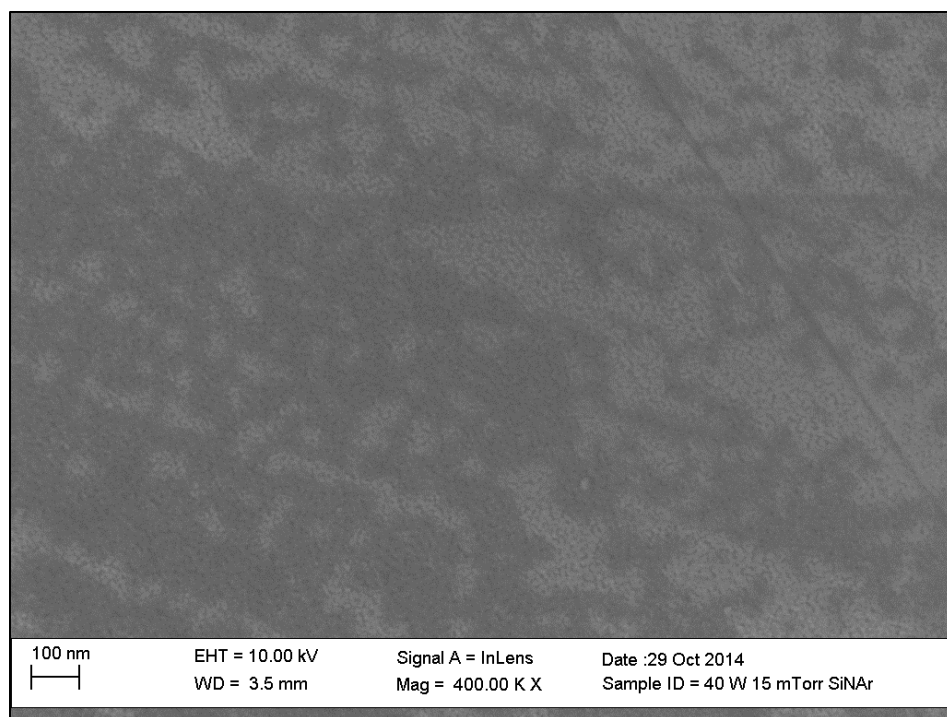
(a)
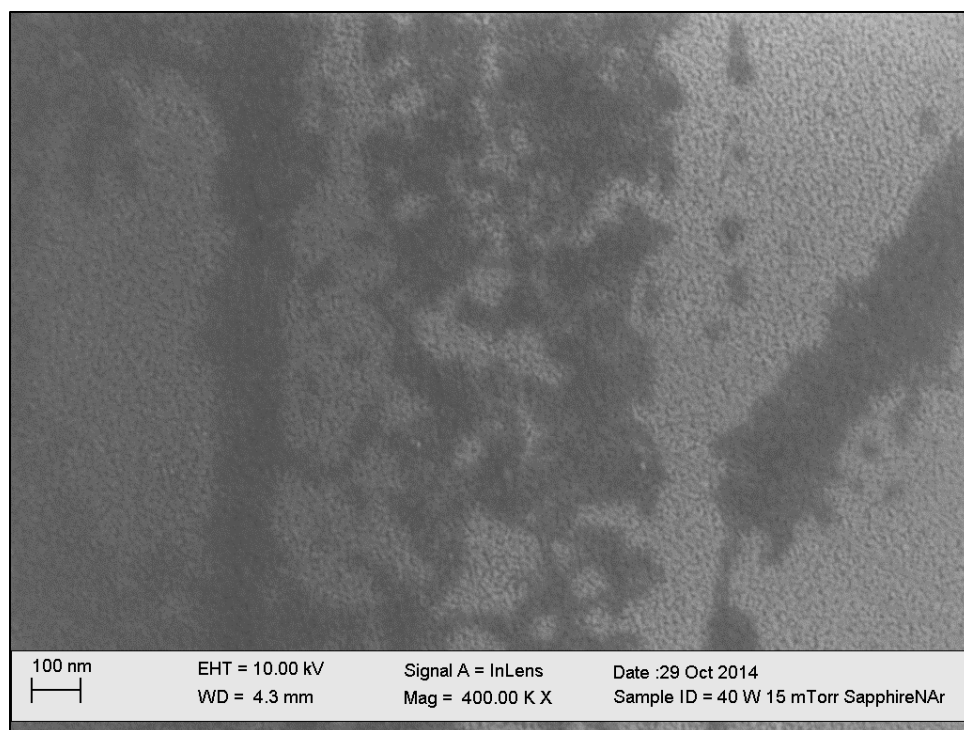
(b)

Figure 5.13 - (a) 40W 15mT Si 15 nm grain, (b) 40W 15mT Sapphire 10 and 15nm using 60% N2

(a)

(b)

Figure 5.14 - (a) 40W 15mT N2 Sapphire LV, ~10nm grain size, (b) 40W 15mT N2 Silicon LV, grain size ~10nm

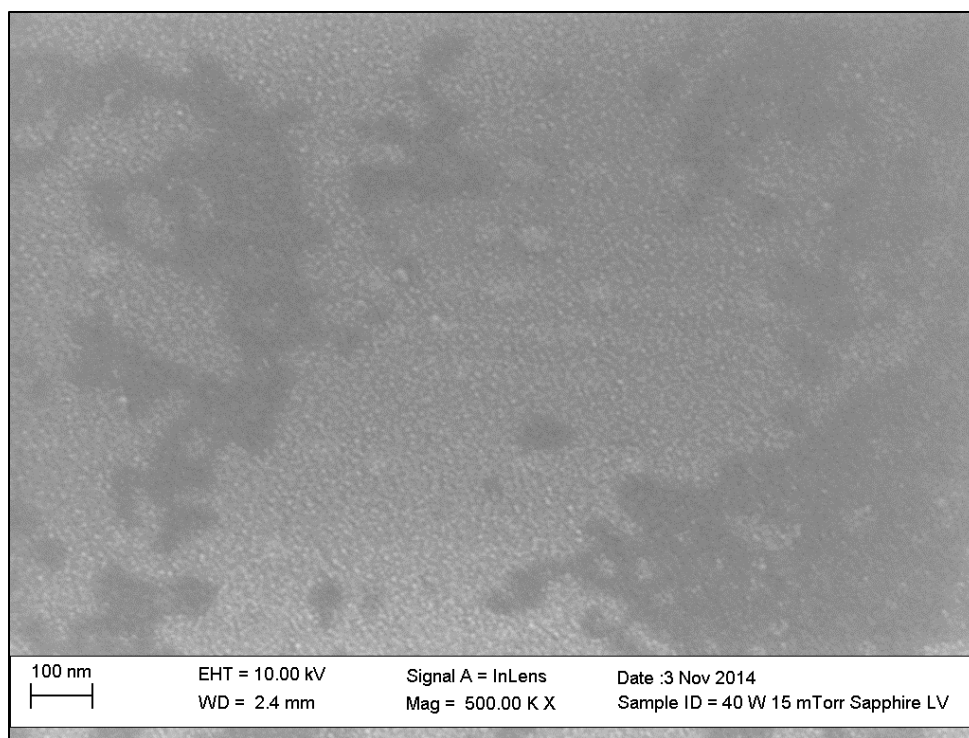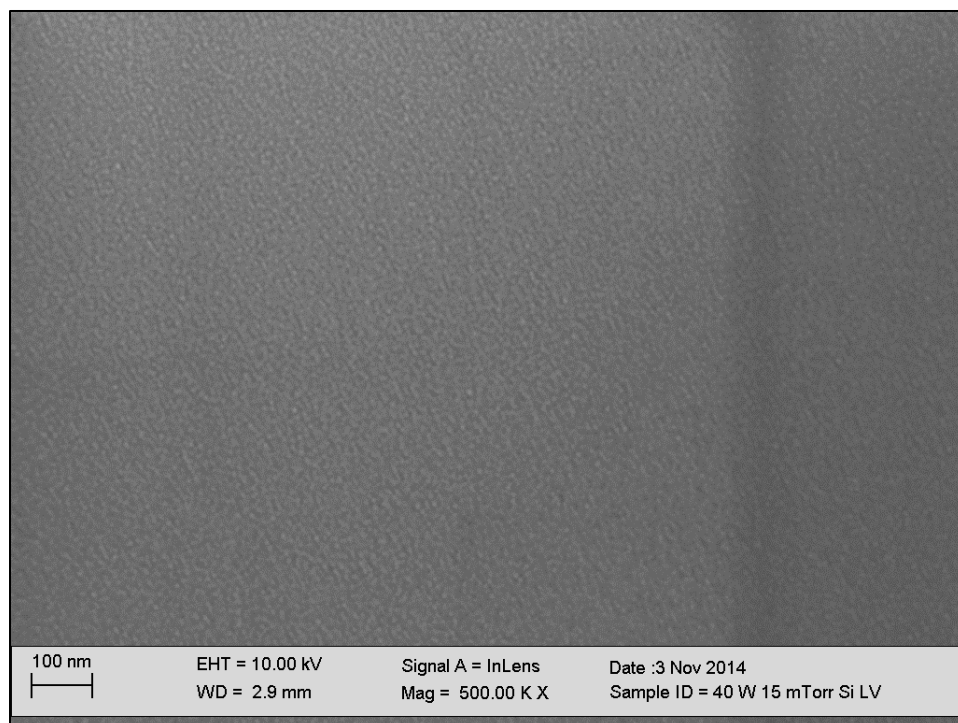| 200 nm | EHT = 10.00 kV | Signal A = InLens | Date :29 Oct 2014 |
| | WD = 4.0 mm | Mag = 400.00 K X | Sample ID = 15 W 15 mTorr SiN |
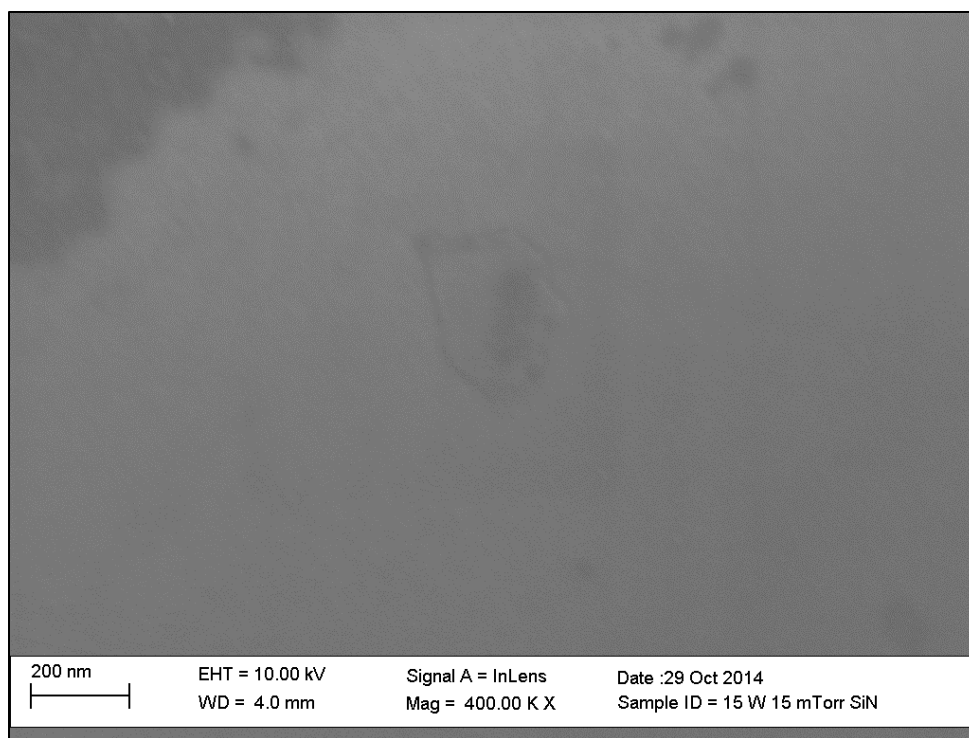
Figure 5.15 - No grains

5.5 Temperature Depositions

Throughout the depositions, oxygen impurities were found on all films. XPS data of the films depicted that the oxygen incorporation for the films was not only at the surface, as was the case for carbon. To reduce any residual oxygen left at the vacuum chamber, the sputtering was done at a base pressure closer to ~10^{-8}. However, this is not enough to reduce oxygen impurities. An increase in temperature does reduce oxygen. In Table 5.8, a decrease in oxygen was clearly seen with high temperature depositions, especially at a temperature of 700°C. The SEM surface images of each film on silicon and sapphire wafers showed clear grain formations of various sizes, Figures 5.16 and 5.17 illustrate depositions done at 400°C and Figures 5.18 and 5.19 for depositions done at 700°C. An increase in grain size due to temperature was clearly seen from an average of 14nm to 50nm. XRD results of the 400°C depositions shown on Figure 5.20 indicated

that crystals were beginning to form. On Figure 5.21, with an increase in temperature and thickness, the peaks of wurtzite of 32.4°, 34.6°, and 36.8° were seen. Some peaks of Ga2O3 are still observed, meaning oxygen has not been completely removed during the deposition. XPS spectrum of binding energies show a peak at 20.5eV for the temperatures grown at 400°C and a peak at 19.8eV for the temperatures grown at 700°C, Figure 5.22. Elemental gallium has a binding energy at 18.7eV. The positive shift to 19.8eV and 20.5eV indicated no elemental gallium. From the peak difference of 400°C and 700°C, the 700°C depositions had a narrower peak of 20.5eV, and wider peak of 19.8eV, meaning there is more GaN present than Ga2O3. In the depositions of 400°C, the wider peak at 20.5eV indicated higher Ga2O3 atoms than GaN. This showed that higher temperatures greatly reduced oxygen impurities.

Table 5.8 - Sputtered films with temperatures of 400°C and 700°C

Nitrogen Gas 40W 5mT							
Wafer	Temperature	Thickness	Atomic percentage			N/Ga	Time
	(°C)	(nm)	Ga (%)	N	O	Ratio	(hrs.)
Silicon	400	40	9.7	9.28	8.77	0.95670103	1
Sapphire	400	40	8.04	7.23	47.32	0.89925373	1
Silicon	700	300	48.09	36.85	6.28	0.76627157	10
Sapphire	700	300	51.35	37.6	6.48	0.7322298	10
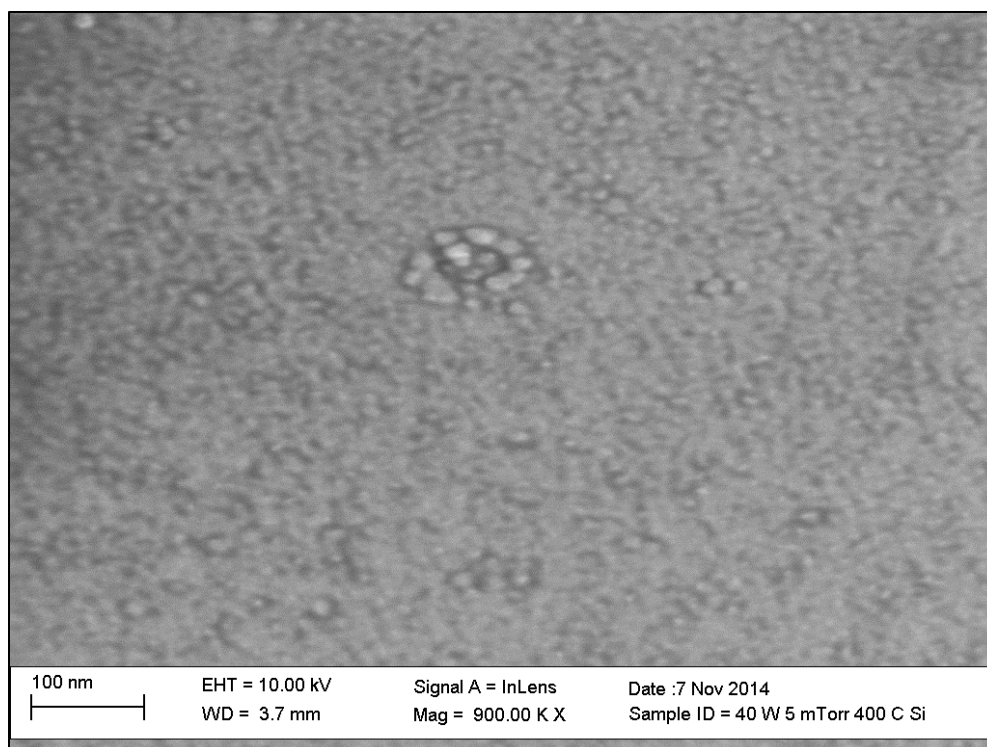
Figure 5.16 - Temperature deposition at 400°C on Silicon, grains (12nm and 15nm)
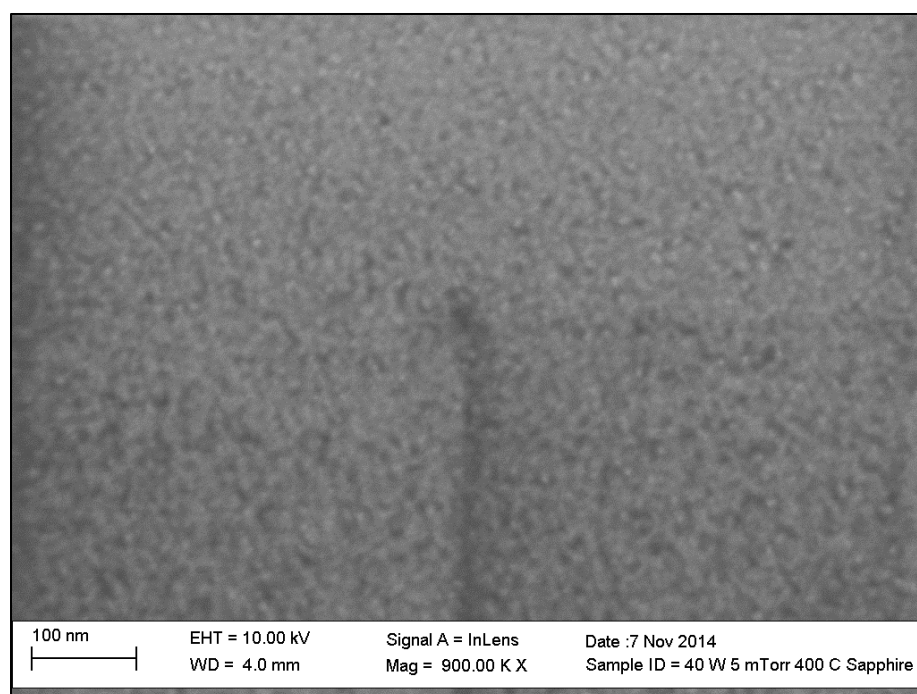
Figure 5.17 - Temperature depositions at 400°C on sapphire (grain sizes 10nm, 14nm)
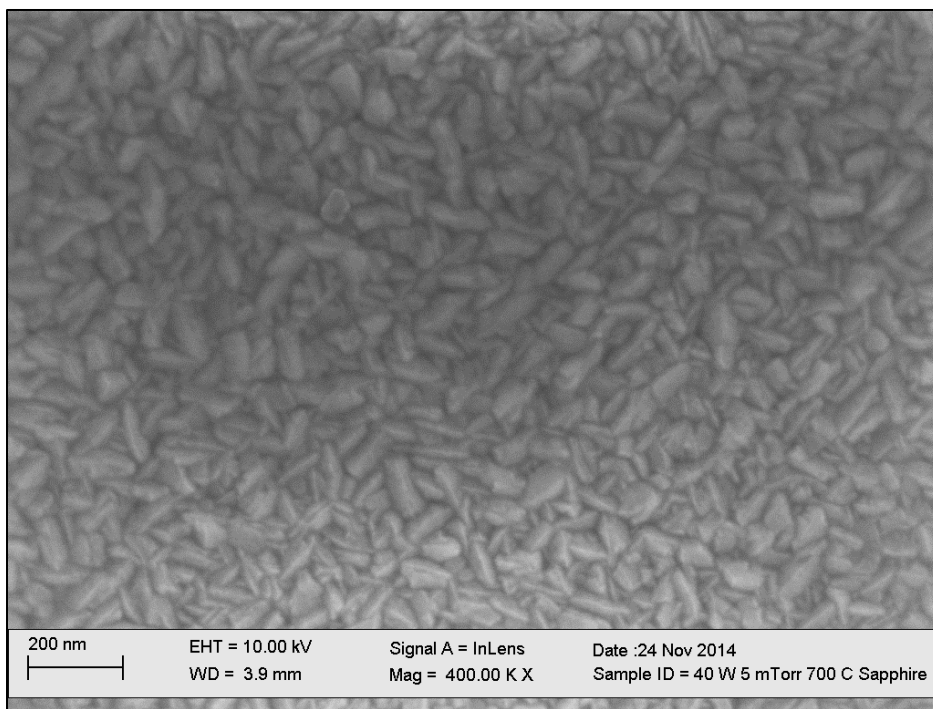
Figure 5.18 - 62nm 39nm grains on sapphire
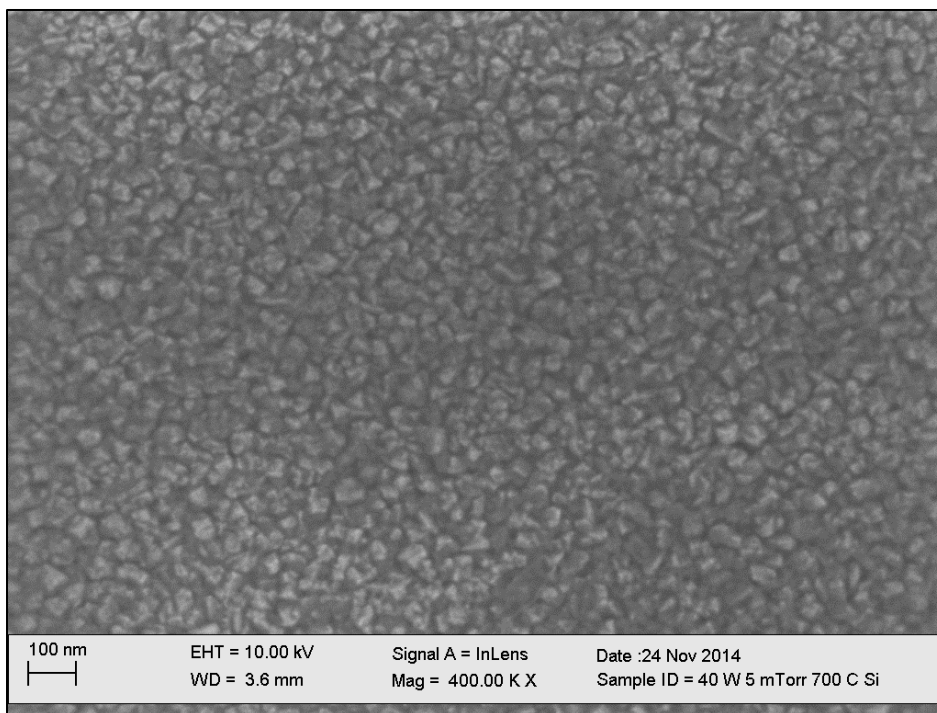
Figure 5.19 - 40nm and 38nm grains on silicon
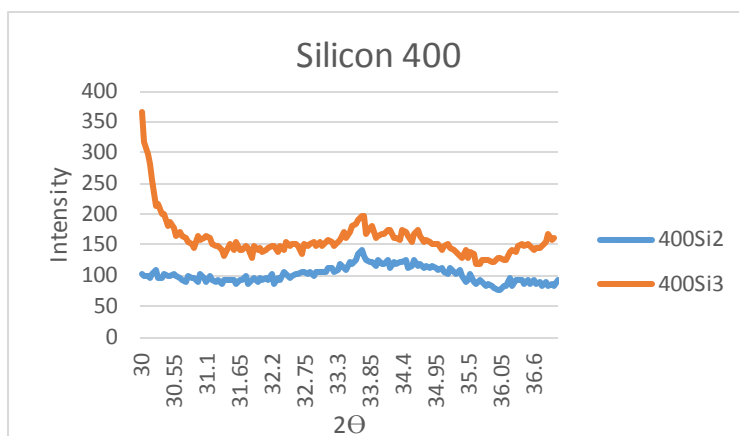
Figure 5.20 - 1hr 400°C 40W 5mT
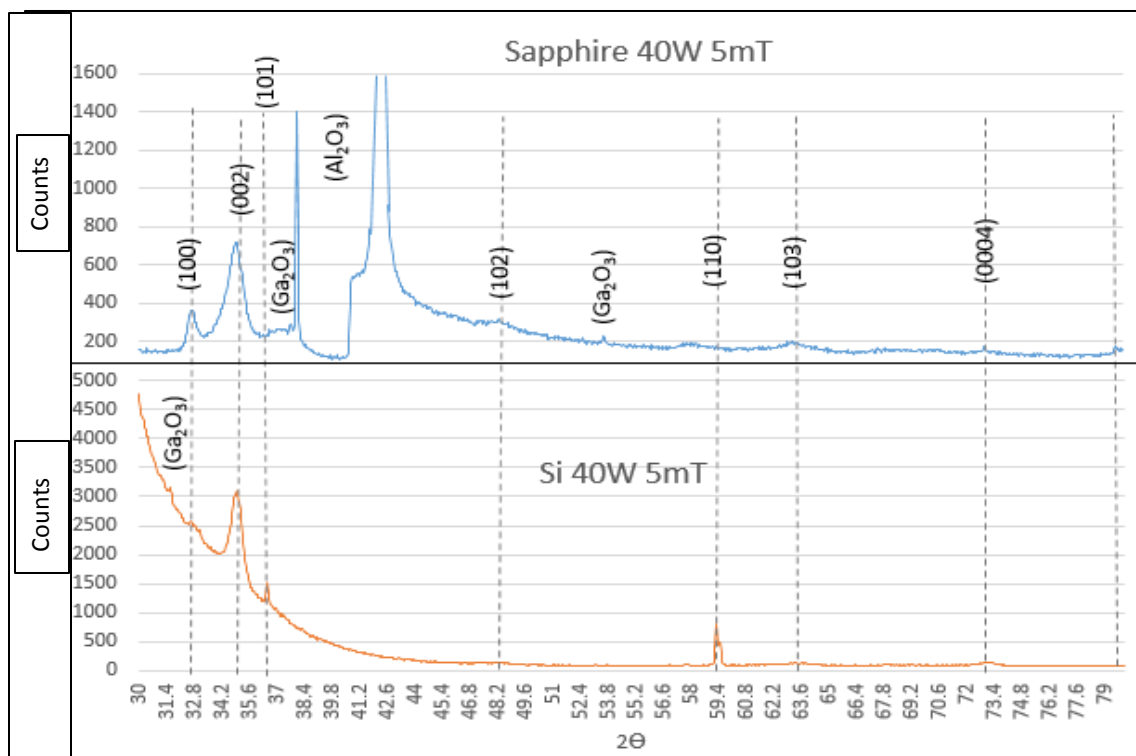
Figure 5.21 - 40W 5mT pure N 700°C
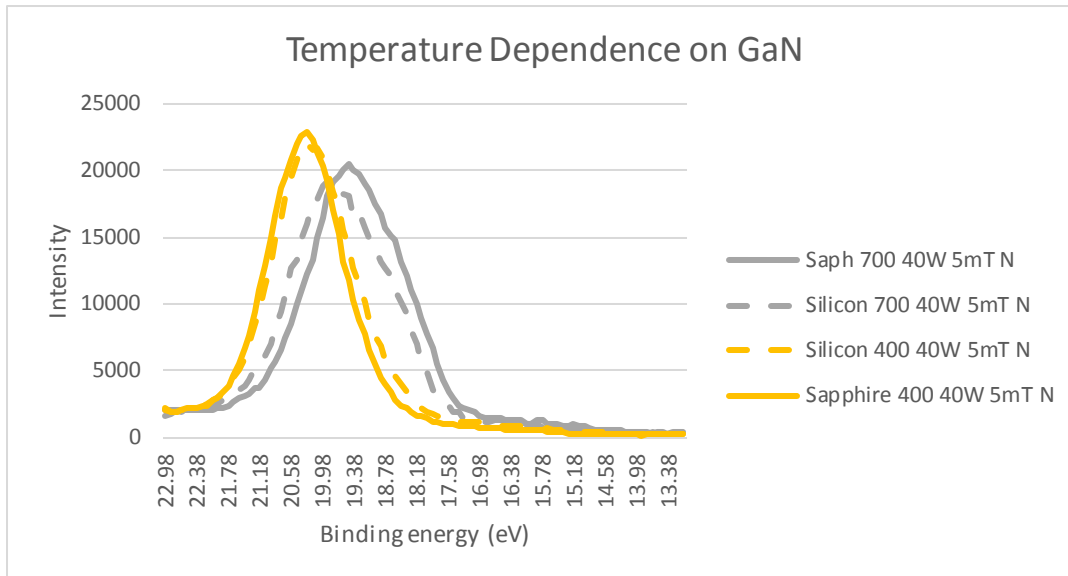
Figure 5.22 - XPS data of Ga 3d binding energy

5.6 Confirmation of the Impurities with XPS

Oxygen and carbon impurities had been revealed by EDS on all of the GaN deposited films. These impurities had first been assumed to be coming from exposure to atmospheric impurities due to not having a clean room environment. Analyzing the films using XPS indicated the impurities of carbon are only found at the surface of the films, as no carbon is detected after etching 0.12nm. As can be seen by Figure 5.23 of selected thin films analyzed by XPS, the oxygen concentration is always higher than gallium, when using a nitrogen/argon gas mix. Only when the depositions are done using pure Ar gas is the gallium atomic concentration higher than oxygen. This is attributed to the argon gas promoting higher kinetic energies of the Ga and N atoms, causing a deflection of oxygen atoms. In Figure 5.24, a reduction in oxygen is seen with increasing temperatures. If impurity atoms of oxygen were observed, the oxygen atoms will replace nitrogen vacancies [53]. When oxygen occupies an N site, it is known as a substitutional impurity and causes point defects. It also presents carbon impurities as being able to replace

nitrogen vacancies, as an amphoteric impurity however the carbon atoms in these films are only at the surface, as is discussed in section 5.1.
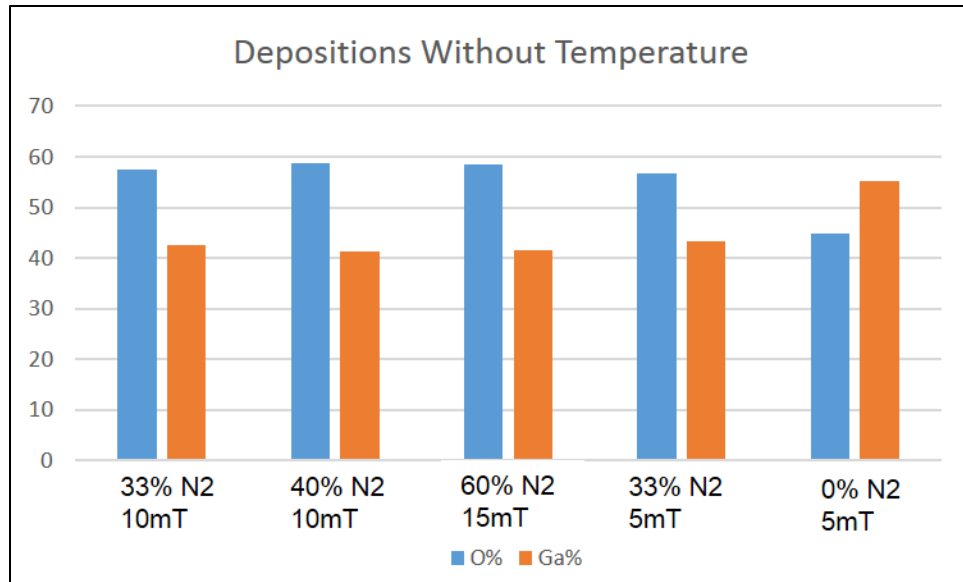
Figure 5.23 - Oxygen impurities at various parameters without temperature
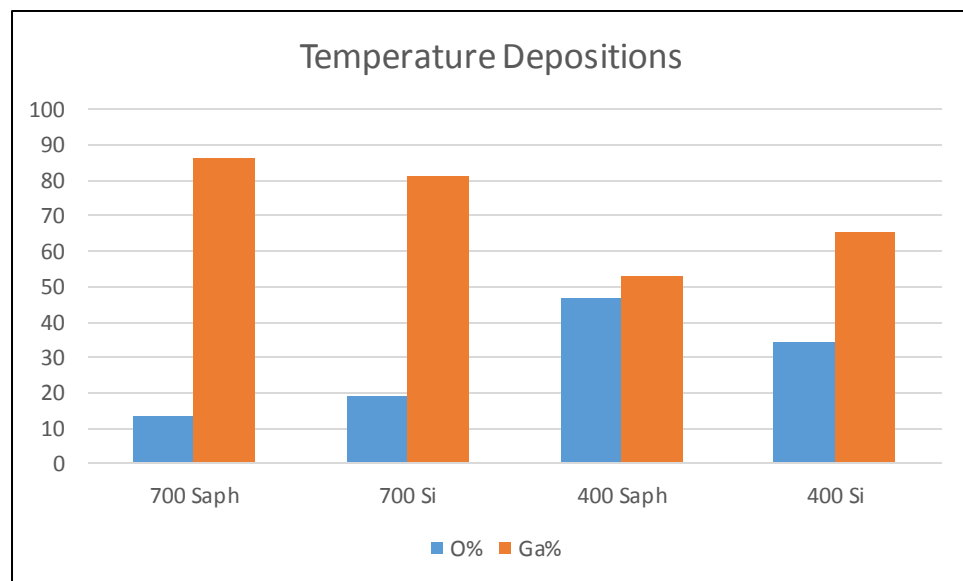
Figure 5.24 - Depositions done using temperature to reduce oxygen concentration

5.7 Target poisoning

Sputtering with an argon flow rate greater than N had an effect on the gallium nitride target. The greatest effect was observed in the pure Argon gas depositions, where the target had a completely black surface. Additionally, at 50W RF power, the effect was greater than at 40W RF power. This can be attributed to the intense bombardment of argon ions causing a resputtering at the surface of the target and leaving the surface nitrogen deficient. This phenomenon is observed when sputtering in pure argon gas in [44]. There is no mention of target poisoning. It is assumed that was occurring both at the target surface as well as the substrate in this Thesis. This was indicated by samples grown at pure argon gas having high gallium content and really low nitrogen. Nitrogen gas is introduced and becomes 60% higher than argon gas, the films become closer to stoichiometric as well as the reduction in target poisoning. The visual inspection at the target surface is shown by Figure 5.25. In Figure 5.25 (a), the black surface layer is seen after the depositions done with pure argon gas. As nitrogen gas is introduced, the effect begins to be suppressed. Sputtering at a 33% N2 with high pressure, even with 50W RF power, the target surface begins to clear (b). Sputtering at low pressures of 4mT or 5mT (c), target poisoning is still observed, and again is greater at 50W RF power (d). Once the sputtering gas is 60% N2 and a higher pressure (10mT or above), Figure (e), this effect begins to be reduced. At 15mT with 60% or higher N2 the target is almost clear of the black material, Figure (f). This was the same results obtained when sputtering below 40W RF power, for the depositions done at 15W RF power. Figure (g) shows the surface of the target with small black specs, this is due to sputtering at a low pressure of 5mT with 40W. At these parameters, the effect is suppressed enough to not cause damage to the sputtered film. The target is found to be the cleanest at RF powers of 40W or below, and pressures of 10mT and above, with 60% N2 flow rate.
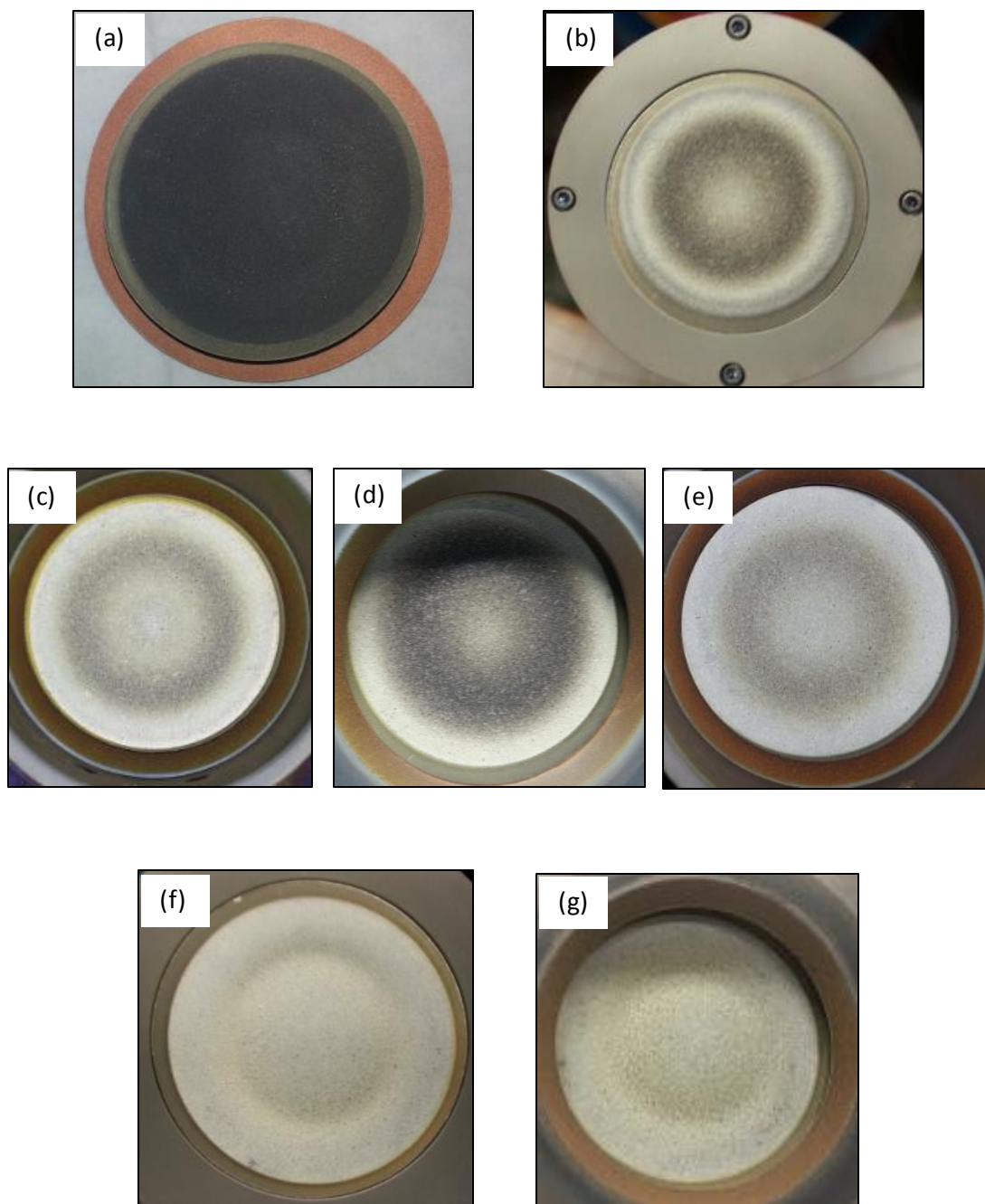
Figure 5.25 - Surface of GaN target, at various parameters: (a) pure Argon gas, (b) 33% N2 40W, (c) 33% N2 high pressures, (d)33% N2 50W low pressures, (e) 40% N2 40W 10mT, (f) 60% N2 and pure N2 40W 15mT, (g) 70% N2 40w 5mT

CHAPTER VI

CONCLUSION AND FUTURE WORKS

6.1 Summary

GaN thin films have been grown by sputtering a GaN target. The sputtering parameters of RF power and pressure are varied to study the effects on the structural properties of the films. Additionally, the sputtering gasses used are argon gas, argon/nitrogen gas mix, and pure nitrogen gas to test the gas dependence on the structural properties of the thin film. To achieve stoichiometric GaN films, low RF power (40W) and high pressure (15mT) are recommended using pure Nitrogen gas. However impurities of oxygen are still incorporated in the films during the depositions. Substrate temperature of 700°C is needed to reduce the oxygen impurities. By using temperature, the reduction in oxygen impurities also allows low pressure deposition of 5mT to create polycrystalline GaN thin film.

Target poisoning has been a major issue throughout the depositions. The initial experiments ran at 50W RF power and low pressures left the surface of the target with a black material. Analysis of the black material by EDS revealed really high atomic percentage of Ga. A resputtering at the target due to the Argon gas is assumed, leaving the surface of the target nitrogen deficient. This is an important phenomenon as the stoichiometry of the films are greatly affected by the "cleanliness" of the target surface. If target poisoning is observed, target cleaning procedures must be done, otherwise the thin films will come out with higher percentages of

gallium. To suppress target poisoning, low powers, high pressures and the use of 60% nitrogen gas or higher are needed.

6.2 Challenges

One of the main challenges in this research is attributed to the characterization techniques. The imaging tools available for analyzing the thin films are typical equipment's used. However, separate attachments/set ups are not available which allow really thin films, less than 500nm thick, to be properly characterized. The XRD technique typically used is grazing incidence XRD in order to suppress the peaks from the substrate and detect the thin film grown above. Grazing incidence is not available, only XRD is available at this university. This made it very time consuming for detection of the GaN peaks. Many tests had to be done to find the right orientation the film grows on the wafer, as well as lowering the power intensity to read at the surface and not penetrate that far in to the substrate. For surface imaging, the samples had to be prepared to be more conductive in order to take clear pictures. This lead to thinking the films are amorphous early in the research since there was no detection of grains. Grain formations are found once the samples are made more conductive. Use of the XPS machine for chemical analysis was not available until the end of this research. The inability to check for crystallography or chemical composition left analysis to be made solely on EDS elemental composition and visual inspection of the color of the thin films. EDS results are useful for detection of the N/Ga ratio, however it cannot analyze if the gallium nitride has formed. (It only reads atomic elements, it cannot detect chemical compositions).

Another challenge is the impurities within the sputtering chamber. Impurities of unwanted elements have a major effect on the quality of the thin films. Thin films are normally grown in clean room enclosures to reduce impurities. There is no clean room enclosure for the

sputtering system, meaning impurities cannot be completely removed. The characterization tools are also not under clean room enclosures which can have another effect on the films. The sputtering gasses are industrial type gasses and not high purity gasses, which could also contribute to impurities.

The last challenge is poor knowledge of the sputtering system. As this system is new, understanding of proper sputtering parameters and knowing the equipment was learned as the research was done. A poor sputtering process led to target breaking and burning, Figure 6.1. None or poor ramping of the target is what caused the target damage. The damage was also found in the sputter gun's magnetic array and copper mesh (Figures 6.2 and 6.3). In addition, there was also a problem with the adaptive pressure controller. The valve sometimes struggled to keep the pressure setting position, and adaptive pressure controller reader indicated the position fluctuated.
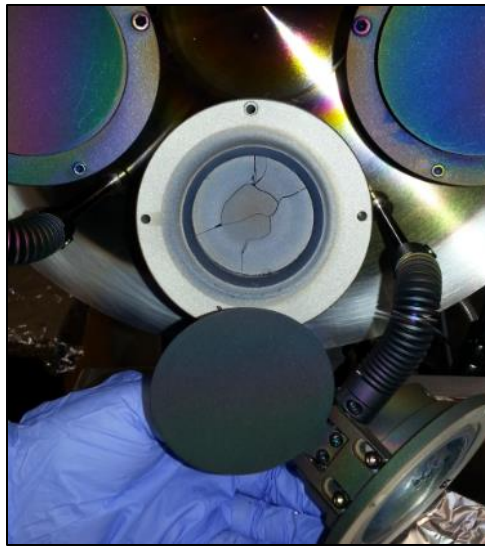
Figure 6.1 - Broken TiO target

Figure 6.2 - Sputter gun's magnet array after TiO deposition
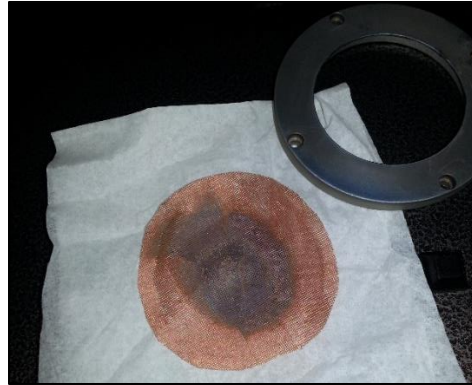
Figure 6.3 - Copper mesh after TiO deposition

6.3 Recommendations and Future Works

Polycrystalline GaN with a wurtzite crystal structure is achieved by this thesis. To achieve a higher quality single crystal structure, further experiments can be done at lower powers and high pressures. As has been reported in [39] single crystal GaN is achieved at 15W and 15mT. This was not fully explored due to time constrains, as running this process to achieve a good thickness could take days. Additionally, oxygen atoms are still found within the deposition. Additional experiments can be done to reduce the oxygen concentrations such as temperature depositions at higher temperatures of 700°C, which was the max temperature used in this Thesis.

Other factors such as post annealing treatments can be done on the film to reduce oxygen atoms. The processing gas used is currently an industrial type gas. High purity nitrogen gas can be used to reduce impurities from the gasses. A negative bias voltage has also been found to be successful in reducing oxygen impurities [54].

To accomplish the overall research for building an AlGaN/GaN HEMT biosensor, the substrate SiC can be used as the substrate and improve the quality of the HEMT. Optimized sputtering conditions of AlGaN still need to be done and characterized. The heterostructure can then be verified, making sure the HEMT works correctly. The use of the HEMT as a biosensor can then be tested (Figure 6.4).
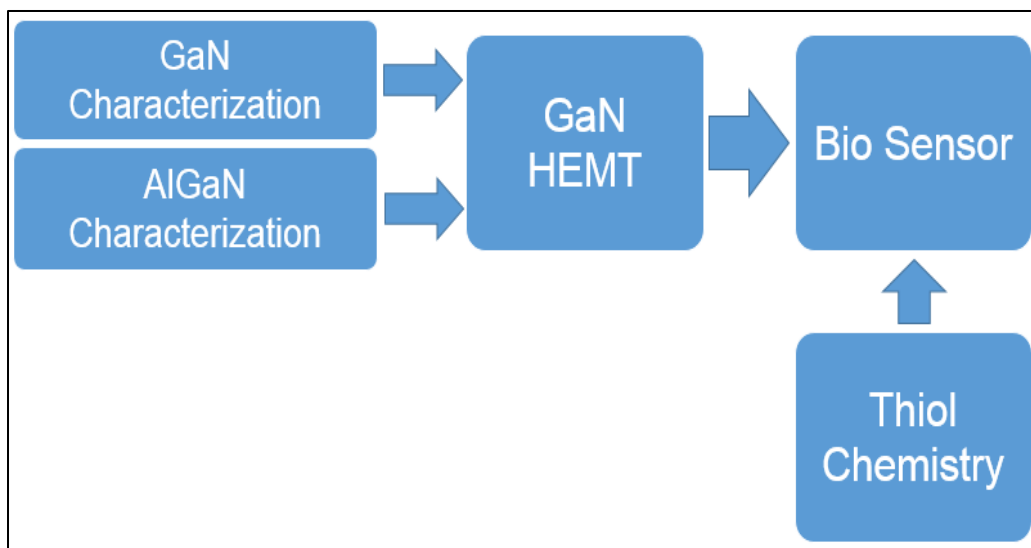
Figure 6.4 – Overall research outline

REFERENCES

[1] W. F. Brinkman,, D. E. Haggan and W. W. Troutman, "A History of the Invention of the Transistor and Where It Will Lead Us," *IEEE Journal of Solid-State Circuits,* vol. 32, no. 12, 1997.

[2] S. Brown and Z. Vrabesic, Fundamentals of Digital Logic with Verilog Design, 2nd ed., McGraw-Hill Science/Engineering/Math, 2007.

[3] F. Ren, S. J. Pearton, B. S. Kang and B. H. Chu, "AlGaN/GaN High Electron Mobility Transistor Based Sensors for Bio-Applications," in *Biosensors for Health, Environment and Biosecurity*, A. Serra, Ed., InTech, 2011.

[4] B. S. Kang, H. T. Wang, F. Ren and S. J. Pearton, "Electrical detection of biomaterials using AlGaN/GaN high electron mobility," *JOURNAL OF APPLIED PHYSICS,* no. 104, 2008.

[5] R. F. Pierret, Advance Semiconductor Fundamentals, Second ed., vol. VI, Prentice Hall, 2002.

[6] S. Choi, E. Heller, D. Dorsey and S. Graham, "The Analysis of Wide Band Gap Semiconductors Using Raman Spectroscopy," in *Materials and Reliability Handbook for Semiconductor Optical and Electron Devices*, 2013, pp. 545-82.

[7] L. Culbertson, "Wide Bandgap Semiconductors Go Beyond Silicon in Power, RF, LED Lighting, and Optoelectronics," Mouser Electronics, [Online]. Available: http://www.mouser.com/applications/. [Accessed 13 September 2014].

[8] Whitaker, Jerry C;, The Electronics Handbook, Second ed., CRC Press, 2005.

[9] "Wide Band Gap Devices: Powering the next Generation of Electric Traction Drive Systems," UT-Battelle for the Dept of Energy.

[10] W. D. Callister, Materials Science and Engineering: An Introduction, Seventh ed., New York: John Wiley & Sons, 2007.

[11] M. Shur and R. F. Davis, GaN-based Materials and Devices: Growth, Fabrication, Characterization and Performance, Singapore: World Scientific, 2004.

[12] S. J. Pearton , C. R. Abernathy and F. Ren, Gallium Nitride Processing for Electronics, Sensors and Spintronics, London: Springer, 2006.

[13] U. K. Mishra, P. Parikh and Y.-F. Wu, "AlGaN/GaN HEMTs: An Overview of Device Operation and Applications," *Proceedings-IEEE,* vol. 90.6, pp. 1022-1031, 2002.

[14] "2014 Nobel prize in Physics — The invention of efficient blue LEDs," Institut NEEL, 2 December 2014. [Online]. Available: http://neel.cnrs.fr/spip.php?article3968&lang=fr. [Accessed 4 December 2014].

[15] A. Agrawal, P. Agrawal, K. Sahni, S. Subhechha, K. Gupta and T. K. Baranwal, "AlGaN/GaN HEMT:AN OVERVIEW OF DEVICE OPERATION, ITS ADVANTAGES AND LIMITATIONS," [Online]. Available: http://www.academia.edu/1863516/TERM_PAPER_EE_311_AlGaN_GaN_HEMT_AN_ OVERVIEW_OF_DEVICE_OPERATION_ITS_ADVANTAGES_AND_LIMITATIONS . [Accessed 14 October 2014].

[16] H. Ye, "Electrical Characterization of GaN:Si and AlGaN:Si," CHALMERS UNIVERSITY OF TECHNOLOGY, Goteborg, 2011.

[17] H. Trevino, "AN ANALYTICAL AND EXPERIMENTAL BIOSENSOR," University of Texas Pan American, Edinburg, 2014.

[18] S. J. Pearton and F. Ren, Semiconductor Device-Based Sensors for Gas, Chemical, and Biomedical Applications, CRC Press, 2011.

[19] D. M. Mattox, The Foundations of Vacuum Coating Technology, Norwich: William Andrew Publishing, 2003.

[20] L. Schultz, "VCD vs PVD," Prezi, 14 January 2014. [Online]. Available: https://prezi.com/iob3wgczzuuz/cvd-vs-pvd/. [Accessed 23 July 2014].

[21] Z. C. Feng, Ed., III-Nitride Devices and Nanoengineering, London: Imperial College Press, 2008.

[22] M. Ohring, Materials Science of Thin Films, 2nd ed., Academic Press, 2001.

[23] K. Wasa, M. Kitabatake and H. Adachi, Thin Film Materials Technology: Sputtering of Compound Materials, Norwich: William Andrew, Inc., 2004.

[24] I. AJA International, "ATC Orion Series UHV Sputtering Systems," AJA International, Inc, 2013.

[25] V. Bhatt, S. Chandra, S. Kumar and C. M. Rauthan, "Stress evaluation of RF sputtered silicon dioxide films for MEMS," *Indian Journal of Pure and Applied Physics,* no. 45, p. 377–381, 2007.

[26] "Semiconductor Electronics:Materials, Devices and Simple Circuits," [Online]. Available: http://ncert.nic.in/NCERTS/l/leph206.pdf. [Accessed 12 October 2014].

[27] C. Honsberg and S. Bowden, "Semiconductor Materials," PV Education.org, [Online]. Available: http://pveducation.org/pvcdrom/pn-junction/band-gap. [Accessed 6 September 2014].

[28] S. Nakamura and R. M. Krames, "History of Gallium Nitride Based Light Emitting Diodes for Illumination," *Proceedings of the IEEE,* vol. 101, no. 10, pp. 2211-2220, 2013.

[29] T. Paskova, Ed., Nitrides with Nonpolar Surfaces: Growth, Properties, and Devices, Weinheim: Wiley-VCH, 2008.

[30] F. Shi, "GaN Nanowires Fabricated by Magnetron Sputtering Deposition," in *Nanowires - Fundamental Research*, A. Hashim, Ed., InTech, 2011.

[31] V. K. Khanna, "Robust HEMT Microsensors as Prospective Successors of MOSFET/ISFET Detectors in Harsh Environments," *Frontiers in Sensors,* vol. I, no. 3, 2013.

[32] F. Fornetti, "Wide Bandgap Semiconductor Materials and Microwave PAs," 16 February 2012. [Online]. Available: https://www.youtube.com/watch?v=GrMs953J0so. [Accessed 8 June 2014].

[33] J. W. Yang, C. J. Sun, Q. Chen, M. Z. Anwar, M. A. Khan, S. A. Nikishin, G. A. Seryogin, A. V. Osinsky, L. Chernyak, H. Temkin, C. Hu and S. Mahajan, "High quality GaN-InGaN heterostructures grown on (111) silicon substrates," *American Institude of Physics,* vol. 96, p. 6951, 1996.

[34] "Gallium Nitride (GaN) versus Silicon Carbide (SiC) in The High Frequency (RF) and Power Switching Applications," Microsemi PPG, [Online]. Available: http://www.digikey.com/Web%20Export/Supplier%20Content/Microsemi_278/PDF/Micr osemi_GalliumNitride_VS_SiliconCarbide.pdf?redirected=1. [Accessed 14 September 2014].

[35] L. Zhang, J. Yu, X. Hao, Y. Wu, Y. Dai, Y. Shao, H. Zhang and . Y. Tian, "Influence of stress in GaN crystals grown by HVPE on MOCVD-GaN/6H-SiC substrate," Scientific Reports, 2014.

[36] C.-W. Wang, B.-S. Soong, J.-Y. Chen, C.-L. Chen and Y.-K. Su, "Effects of gamma-ray irradiation on the microstructural and luminescent," *Journal of Applied Physics,* vol. 88, no. 11, pp. 6355-6358, 2000.

[37] H. W. Kim and . N. H. Kim, "Preparation of GaN films on ZnO buffer layers by," *Applied Surface Science ,* pp. 192-197, 2004.

[38] J. H. Kim, M. R. Davidson and P. H. Holloway, "Electroluminescence from Tm-doped GaN deposited by radio-frequency," *Applied Physics Letters,* vol. 83, no. 23, pp. 4746-4748, 2003.

[39] J. H. Kim and K. Y. Cho, "Structure and Properties of Gallium Nitride Thin Films Deposited on Si (111) by using Radio-Frequency Magnetron Sputtering," *Journal of the Korean Physical Society,* vol. 62, no. 4, pp. 619-622, 2013.

[40] G. Devaraju, P. A. Pathak, N. S. Rao, S. V., S. N. Rao and A. I. Titov, "Synthesis and tailoring of GaN nanocrystals at room," *Radiation Effects & Defects in Solids,* vol. 167, no. 9, pp. 659-665, 2012.

[41] T. Miyazaki, K. Takada and S. Adachi, "Properties of radio-frequency-sputter-deposited GaN films," *Journal of Applied Physics,* p. 97, 2005.

[42] T. Miyazaki , T. Fujimaki and A. Sadao , "Properties of GaN films deposited on Si,,111… by radio-frequency-magnetron," *Journal of Applied Physics,* vol. 89, no. 12, pp. 8316-8320, 2001.

[43] C. W. Zou, M. L. Yin, M. Li, C. S. Liu, L. P. Guo and D. J. Fu, "GaN films deposited on glass substrate by middle-frequency magnetron sputtering," *Thin Solid Films ,* pp. 670-673, 2008.

[44] T. Maruyama and H. Miyake, "Gallium Nitride Thin Films Deposited by Radio-Frequency Magnetron Sputtering," *Journal of Vacuum Science and Technology,* p. 1096, 2006.

[45] A. N. Blaut-Blachev, "Polycrystalline Films of Gallium Nitride," *Semiconductors ,* vol. 35, no. 6, pp. 688-689, 2000.

[46] R. H. Horng, D. S. Wuu, S. C. Wei, S. H. Chan and C. Y. Kung, "A research on the persistent photoconductivity behavior of GaN thin films deposited by r.f. magnetron sputtering," *Thin Solid Films,* pp. 343-344, 1999.

[47] D. M. G. Leite, A. L. J. Pereira, L. F. da Silva and J. H. Dias , "Nanocrystalline GaN and GaN:H Films Grown by RF-Magnetron Sputtering," *Brazilian Journal of Physics,* vol. 36, no. 3B, 2006.

[48] "AJA International, Inc.," [Online]. Available: http://www.ajaint.com/. [Accessed 4 April 2014].

[49] "Practical Process Tips," Summer 2010. [Online]. Available: http://www.lesker.com/leskertech/archives/0g11m3h/leskertech_v7_i1.pdf. [Accessed 15 May 2014].

[50] V. Kadir , "STRUCTURAL AND MAGNETIC PROPERTIES OF Si(100)/Ta/Co MULTILAYERS FOR SPINTRONICS APPLICATIONS," Izmir Institure of Technology, 2007.

[51] "X-ray Diffraction and Elemental Analysis," Bruker Corporation, 2014. [Online]. Available: http://www.bruker.com/products/x-ray-diffraction-and-elemental-analysis.html. [Accessed 2 September 2014].

[52] "XPS Reference: Gallium," Thermo Fisher Scientific Inc., 2013. [Online]. Available: http://xpssimplified.com/elements/gallium.php#aboutthiselement. [Accessed 1 November 2014].

[53] F. K. Yam, . L. . L. Low, S. A. Oh and Z. Hassan, "Gallium Nitride: An Overview of Structural Defects," in *Optoelectronics - Materials and Techniques*, P. P. Predeep, Ed., InTech, 2011.

[54] H. M. . I. Jaim, . J. . A. Aguilar, . B. Sarabi, Y. J. Rosen, A. N. Ramanayaka, E. H. Lock, C. J. K. Richardson and K. D. Osborn, "Superconducting TiN Films Sputtered over a Large," [Online]. Available: http://arxiv.org/ftp/arxiv/papers/1408/1408.3177.pdf. [Accessed 29 November 2014].

APPENDIX

APPENDIX A

GLOSSARY

Band gap – energy difference between the top of the valance gap and the bottom of the conduction band that an electron has to "jump" and break free to become a charge carrier [27]

Conduction band – lowest energy band where electrons reside that have been excited to that state and are "free electrons" [10]

Covalent bond – a chemical bond that occurs when two atoms share an electron pair [27]

Crystal structure – the periodic arrangement of atoms in space found in crystalline materials [10]

Point defects – defects around a single lattice point that involve a few extra or missing atoms. It can introduce internal strain which is either compressive or tensile depending on the size of the impurity atom [53]

Substitutional impurity – a point defect, where an impurity atom will replace the site of a bulk atom [53]

Target max power – maximum power applied to the target which is dependent on the target's thermal conductivity, thermal coefficient of expansion [49]

Valance band – the highest electron energy band containing valance electrons [10]

Vacancy – An unoccupied regular crystal site is called a vacancy [53]

BIOGRAPHICAL SKETCH

Rocio Yolanda Garza was born in Monterrey, Mexico in 1988. She is the daughter of Lourdes Mantecon-Garza, a medical doctor and freelance writer, and Jesus Miguel Garza, an MD with a specialty in Family Medicine. She is the youngest of four sisters. When she was 8 years old, she moved with her family to McAllen, TX. She has spent her life living in South Texas since. In her free time, she loves to play basketball, watch movies and TV shows, and travel whenever she can. Rocio received her Bachelor's degree from the University of Texas-Pan American in May 2011 and her Master's degree in December 2014. She is a member of multiple organizations: the Institute of Electrical and Electronics Engineers (IEEE), Mexican American Scientist and Engineers (MAES), Tau Beta Pi, and Kappa Delta Chi, Sorority Inc. She also participated in the IEEE Region 5 Robotics Conference in 2011. Her main research interest are solid state device physics with an emphasis on sputter grown GaN thin film for preparation of an AlGaN/GaN HEMT based biosensor. She maintained a 3.9 average throughout her graduate career and conducted multiple experiments for optimization of growth conditions of GaN thin film. Upon graduation from the University of Texas-Pan American, Rocio is to join IBM in Austin, Texas as a Hardware Development Engineer for the Power Systems Characterization group.

Permanent address: 1400 W. Gardenia McAllen, TX 78501

Permanent email address: rygm00@yahoo.com